C-2

Interaction Notes

Note 195

December 1970

THEORY AND COMPUTATION OF CHARACTERISTIC MODES FOR CONDUCTING BODIES

by

Roger F. Harrington
Joseph R. Mautz

Syracuse University
Syracuse, New York 13210

ABSTRACT

A theory of characteristic modes for conducting bodies is developed starting from the operator formulation for the current. The mode currents form a weighted orthogonal set over the conductor surface, and the mode fields form an orthogonal set over the sphere at infinity. It is shown that the modes are the same ones introduced by Garbacz to diagonalize the scattering matrix of the body. Formulas for the use of these modes in antenna and scatterer problems are given. A procedure for computing the characteristic modes for bodies of arbitrary shape is developed, and applied to conducting bodies of revolution and to wire objects. Illustrative examples of the computation of characteristic currents and characteristic fields are given for a cone-sphere, a disk, and a wire arrow. Modal solutions using these modes are computed for representative antenna and scattering problems to illustrate convergence of the solution as the number of modes is increased. For electrically small and intermediate size bodies, only a few modes are needed to characterize the electromagnetic behavior of the body.

CONTENTS

PART 1

GENERAL THEORY

I. INTRODUCTION

Characteristic modes have long been used in the analysis of radiation and scattering by conducting bodies whose surfaces coincide with coordinate surfaces of coordinate systems in which the Helmholtz equation is separable. Recently Garbacz [1] has shown that similar modes can be defined for conducting bodies of arbitrary shape. He approached the problem by diagonalizing the scattering matrix. This led him to the conclusion that the mode currents are real, and the tangential electric mode field is of constant phase over the surface of the body. Garbacz, Turpin, and Wickliff [1,3,4] used this property to find the characteristic currents in a few cases, but they did not obtain convenient formulas for computing the mode currents in general.

In this report we approach the problem from the alternative viewpoint of diagonalizing the operator relating the current to the tangential electric field on the body. By choosing a particular weighted eigenvalue equation, we obtain the same modes as defined by Garbacz. Our approach leads to a simpler derivation of the theory, and to explicit formulas for determining the mode currents and fields. Also, we consider both near and far fields, whereas Garbacz considered only far field patterns.

II. CHARACTERISTIC CURRENTS

Consider the problem of one or more conducting bodies, defined by the surface S, in an impressed electric field $\vec{E}^i$. An operator equation for the current $\vec{J}$ on S is [6]

$$[L(\vec{J}) - \vec{E}^i]_{tan} = 0 \qquad (1\text{-}1)$$

where the subscript "tan" denotes the tangential components on S. The operator L is defined by

$$L(\vec{J}) = j\omega \vec{A}(\vec{J}) + \vec{\nabla}\Phi(\vec{J}) \tag{1-2}$$

$$A(\vec{J}) = \mu \iint_S \vec{J}(\vec{r}')\ \psi(\vec{r},\vec{r}')ds' \tag{1-3}$$

$$\Phi(\vec{J}) = \frac{-1}{j\omega\varepsilon} \iint_S \nabla' \cdot \vec{J}(\vec{r}')\ \psi(\vec{r},\vec{r}')ds' \tag{1-4}$$

$$\psi(\vec{r},\vec{r}') = \frac{e^{-jk|\vec{r}-\vec{r}'|}}{4\pi|\vec{r}-\vec{r}'|} \tag{1-5}$$

Here $\vec{r}$ denotes a field point, $\vec{r}'$ a source point, and ε,μ,k the permittivity, permeability, wavenumber, respectively, of free space. Physically, $-L(\vec{J})$ gives the electric intensity $\vec{E}$ at any point in space due to the current $\vec{J}$ on S. In an antenna problem, the impressed field $\vec{E}^i$ is the negative of the tangential component of $\vec{E}$ over S, assumed known. In a scattering problem, the impressed field $\vec{E}^i$ is due to known sources external to S.

We define the symmetric product of two vector functions $\vec{B}$ and $\vec{C}$ on S as

$$\langle B,C\rangle = \iint_S \vec{B} \cdot \vec{C}\ ds \tag{1-6}$$

The product $\langle B^*,C\rangle$, where * denotes complex conjugate, defines an inner product for the complex Hilbert space of all square-integrable vector functions on S. The operator appearing in (1-1) has the dimensions of impedance, and we introduce the notation

$$Z(\vec{J}) = [L(\vec{J})]_{tan} \tag{1-7}$$

That Z is a symmetric operator, i.e., $\langle B,ZC\rangle = \langle ZB,C\rangle$, follows from the reciprocity theorem [5]. However, Z is not a Hermitian operator, i.e., $\langle B^*,ZC\rangle \neq \langle Z^*B^*,C\rangle$. Because Z is symmetric, its Hermitian parts are real and given by

$$R = \frac{1}{2}(Z + Z^*) \tag{1-8}$$

$$X = \frac{1}{2j}(Z - Z^*) \tag{1-9}$$

Now $Z = R + jX$ where R and X are real symmetric operators. Furthermore, R is positive semidefinite, since the power radiated by a current $\vec{J}$ on S is $\langle J^*, RJ \rangle \geq 0$. If no resonator fields exist internal to S, then R is positive definite, i.e., all currents radiate some power, however small.

Next consider the eigenvalue equation

$$Z(\vec{J}_n) = \nu_n M(\vec{J}_n) \tag{1-10}$$

where ν_n are eigenvalues, $\vec{J}_n$ are eigenfunctions, and M is a weight operator to be chosen. The eigenfunctions for any choice of symmetric M will diagonalize Z, but only the choice M = R also gives orthogonality of the radiation patterns. (The choice M=I, the identity operator, is considered in Appendix A.) Hence, we choose M = R and set $Z = R + jX$ in (1-10), obtaining

$$(R + jX)(\vec{J}_n) = \nu_n R(\vec{J}_n) \tag{1-11}$$

It is evident that the real part of ν_n must be unity, and we set

$$\nu_n = 1 + j\lambda_n \tag{1-12}$$

where λ_n is real. The common term $R(\vec{J}_n)$ in (1-11) can now be cancelled, giving

$$X(\vec{J}_n) = \lambda_n R(\vec{J}_n) \tag{1-13}$$

Both X and R are real symmetric operators. Hence, all eigenvalues λ_n and eigenfunctions $\vec{J}_n$ must be real. The $\vec{J}_n$ must also satisfy the usual orthogonality relationships

$$\left.\begin{aligned} \langle J_m, RJ_n \rangle &= 0 \\ \langle J_m, XJ_n \rangle &= 0 \\ \langle J_m, ZJ_n \rangle &= 0 \end{aligned}\right\} \; m \neq n \tag{1-14}$$

Furthermore, since the $\vec{J}_n$ are real, the orthogonality relationships are also valid for inner products, that is,

$$\left.\begin{aligned} \langle J_m^*,\ RJ_n \rangle &= 0 \\ \langle J_m^*,\ XJ_n \rangle &= 0 \\ \langle J_m^*,\ ZJ_n \rangle &= 0 \end{aligned}\right\} m \neq n \qquad (1\text{-}15)$$

The choice of $\{\vec{J}_n\}$ as basis functions therefore simultaneously leads to diagonal matrix representations of R, X, and Z. We shall call these $\vec{J}_n$ the characteristic currents or eigencurrents of the conducting body defined by S.

So far the eigencurrents are of indeterminate amplitude. Each eigencurrent which radiates can be normalized according to

$$\langle J_n^*,\ RJ_n \rangle = 1 \qquad (1\text{-}16)$$

i.e., it radiates unit power. Each eigencurrent associated with an internal resonance cannot be so normalized, but they are not needed for radiation problems. When normalized according to (1-16), the orthogonality relationships (1-14) and (1-15) can be combined with (1-16) to give

$$\begin{aligned} \langle J_m, RJ_n \rangle &= \langle J_m^*,\ RJ_n \rangle = \delta_{mn} \\ \langle J_m, XJ_n \rangle &= \langle J_m^*,\ XJ_n \rangle = \lambda_n \delta_{mn} \\ \langle J_m, ZJ_n \rangle &= \langle J_m^*,\ ZJ_n \rangle = (1+j\lambda_n)\delta_{mn} \end{aligned} \qquad (1\text{-}17)$$

where δ_{mn} is the Kronecker delta (0 if $m \neq n$ and 1 if $m=n$). For further theory we assume the eigencurrents to be normalized. If unnormalized currents are used, the factor $\langle J_n,\ RJ_n \rangle$ must be properly introduced into the theory.

III. CHARACTERISTIC FIELDS AND PATTERNS

The electric field $\vec{E}_n$ and the magnetic field $\vec{H}_n$ produced by an eigencurrent $\vec{J}_n$ on S will be called the characteristic fields or eigenfields corresponding to $\vec{J}_n$. The set of all $\vec{E}_n$ or $\vec{H}_n$ form a Hilbert space of all fields throughout space produced by currents on S. We obtain orthogonality

relationships for the characteristic fields from those for characteristic currents by means of the complex Poynting theorem [5]. Explicitly, the complex power balance for currents $\vec{J}$ on S is given by

$$P = \langle J^*, ZJ \rangle = \langle J^*, RJ \rangle + j \langle J^*, XJ \rangle$$

$$= \oiint_{S'} \vec{E} \times \vec{H}^* \cdot d\vec{s} + j\omega \iiint_{\tau'} (\mu \vec{H} \cdot \vec{H}^* - \varepsilon \vec{E} \cdot \vec{E}^*) d\tau \qquad (1\text{-}18)$$

where S' is any surface enclosing S and τ' is the region enclosed by S'. Equation (1-18) is a Hermitian quadratic form, for which the associated Hermitian bilinear form is

$$P(\vec{J}_m, \vec{J}_n) = \langle J_m^*, ZJ_n \rangle \qquad (1\text{-}19)$$

If $\vec{J}_m$ and $\vec{J}_n$ are eigencurrents, then the orthonormality relationships (1-17) apply, and we have from (1-18) and Maxwell's equations

$$\oiint_{S'} \vec{E}_m \times \vec{H}_n^* \cdot d\vec{s} + j\omega \iiint_{\tau'} (\mu \vec{H}_m \cdot \vec{H}_n^* - \varepsilon \vec{E}_m \cdot \vec{E}_n^*) d\tau = (1 + j\lambda_n)\delta_{mn} \qquad (1\text{-}20)$$

This equation can be separated into real and imaginary parts to give orthogonality relationships similar to the first two of (1-17), if desired.

If the body S is of finite extent, and if S' is chosen to be the sphere at infinity (S_∞ of Figure 1-1), then (1-20) gives orthogonality relationships for radiation patterns and fields. On S_∞ the characteristic fields are of the form of outward traveling waves, i.e.

$$\vec{E}_n = \eta \vec{H}_n \times \vec{n} = \frac{-j\omega\mu}{4\pi r} e^{-jkr} \vec{F}_n(\theta, \phi) \qquad (1\text{-}21)$$

Here $\eta = \sqrt{\mu/\varepsilon}$ is the intrinsic impedance of space, $\vec{n}$ is the unit radial vector on S_∞, and (θ, ϕ) are the angular coordinates of position on S_∞. The complex vector $\vec{F}_n$ of (1-21) is called the <u>characteristic pattern</u> or <u>eigenpattern</u> corresponding to the eigencurrent $\vec{J}_n$. Adding (1-20) to its conjugate, we find that

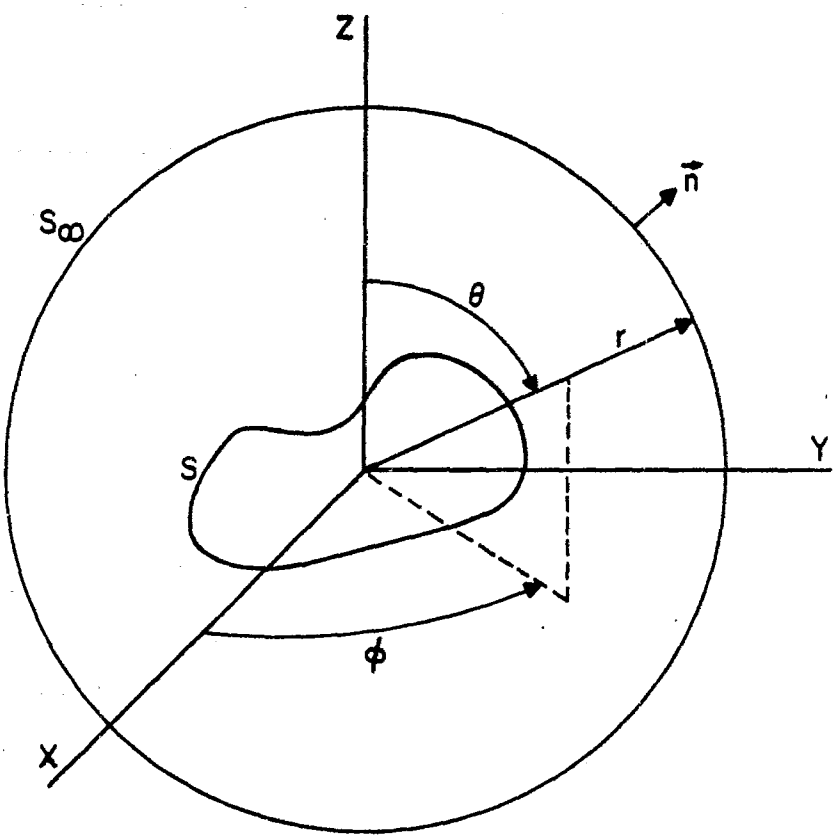

Fig. 1-1. Surfaces and coordinates.

$$\frac{1}{\eta}\oiint_{S_\infty} \vec{E}_m \cdot \vec{E}_n^* ds = \delta_{mn} \tag{1-22}$$

Hence, the characteristic far fields form an orthonormal set in the Hilbert space of all square-integrable vector functions on S_∞. We can also express (1-22) in terms of the characteristic magnetic field as

$$\eta \oiint_{S_\infty} \vec{H}_m \cdot \vec{H}_n^* ds = \delta_{mn} \tag{1-23}$$

Finally, subtracting (1-20) from its conjugate, we obtain the orthogonality relationship

$$\omega \iiint (\mu \vec{H}_m \cdot \vec{H}_n^* - \varepsilon \vec{E}_m \cdot \vec{E}_n^*) d\tau = \lambda_n \delta_{mn} \tag{1-24}$$

where the integration extends over all space. For m=n, equation (1-24) states that λ_n is 2ω times the total stored magnetic energy minus the total stored electric energy. (This assumes that $\langle J_n, RJ_n \rangle = 1$.)

IV. MODAL SOLUTIONS

A modal solution for the current $\vec{J}$ on a conducting body can be obtained by using the eigencurrents as both expansion and testing functions in the method of moments [6]. Following this procedure, we assume $\vec{J}$ to be a linear superposition of the mode currents

$$\vec{J} = \sum_n \alpha_n \vec{J}_n \tag{1-25}$$

where the α_n are coefficients to be determined. Substituting (1-25) into the operator equation (1-1), and using the linearity of L, we obtain

$$[\sum_n \alpha_n L\vec{J}_n - \vec{E}^i]_{tan} = 0 \tag{1-26}$$

Next the inner product of (1-26) with each $\vec{J}_m$ in turn is taken, giving the set of equations

$$\sum_n \alpha_n \langle J_m , ZJ_n \rangle - \langle J_m, E^i \rangle = 0 \tag{1-27}$$

$m=1,2,\ldots$. Here we have put $L_{tan} = Z$, and dropped the subscript "tan" on $\vec{E}^i$. Because of the orthogonality relationship (1-17), equations (1-27) reduce to

$$\alpha_n(1 + j\lambda_n) = \langle J_n, E^i \rangle \tag{1-28}$$

The right-hand side of (1-28) is called the <u>modal excitation coefficient</u>

$$V_n^i = \langle J_n, E^i \rangle = \oiint_S \vec{J}_n \cdot \vec{E}^i ds \tag{1-29}$$

Substituting for α_n from (1-28) into (1-25), we have the modal solution for the current J on S

$$\vec{J} = \sum_n \frac{V_n^i \vec{J}_n}{1+j\lambda_n} \tag{1-30}$$

If the eigencurrents J_n are not normalized according to (1-16), the term $1+j\lambda_n$ in (1-30) should be replaced by $(1+j\lambda_n) \langle J_n, RJ_n \rangle$.

The characteristic fields are linearly related to the characteristic currents, and hence can also be expressed in modal form. Explicitly, these forms are

$$\vec{E} = \sum_n \frac{V_n^i \vec{E}_n}{1+j\lambda_n} \tag{1-31}$$

$$\vec{H} = \sum_n \frac{V_n^i \vec{H}_n}{1+j\lambda_n} \tag{1-32}$$

where $\vec{E}$ and $\vec{H}$ are the fields from $\vec{J}$ everywhere in space. Again, if the eigencurrents are not normalized, the term $1+j\lambda_n$ must be replaced by $(1+j\lambda_n) \langle J_n, RJ_n \rangle$.

Finally, if the reciprocity theorem [5] is used, alternative expressions for the modal excitation coefficients are obtained. For example, if $\vec{E}^i$ is produced by an electric current $\vec{J}^i$, then reciprocal to (1-29) we have

$$V_n^i = \iiint \vec{E}_n \cdot \vec{J}^i d\tau \tag{1-33}$$

where the integration extends over the impressed currents. Similarly, if $\vec{E}^i$ is produced by a magnetic current $\vec{M}^i$, then reciprocal to (1-29) we have

$$V_n^i = -\iiint \vec{H}_n \cdot \vec{M}^i d\tau \tag{1-34}$$

More generally, if $\vec{E}^i$ is produced by both electric currents $\vec{J}^i$ and magnetic currents $\vec{M}^i$ then V_n^i is given by the sum of (1-33) and (1-34).

V. LINEAR MEASUREMENTS

Any scalar ρ linearly related to the current, i.e., a linear functional of the current, will be called a linear measurement of the current. Some examples of linear measurements are (a) a component of the current at some point on S, or (b) a component of the field ($\vec{E}$ or $\vec{H}$) at some point in space. Every linear functional of $\vec{J}$ can be expressed as

$$\rho = \langle E^m, J \rangle \tag{1-35}$$

where $\vec{E}^m$ is a given vector function, usually an electric field on S. For example, if ρ is the j-th component of the field E_j^J from $\vec{J}$, then (1-35) becomes [5,6]

$$E_j^J = \langle E^j, J \rangle \tag{1-36}$$

where $\vec{E}^j$ is the electric field on S produced by a j-directed electric dipole $I\ell = 1$ placed at the field point. If the j-th component of $\vec{H}$ were desired, then a unit magnetic dipole would be placed at the field point, and so on.

If the modal solution (1-30) is substituted into the general measurement formula (1-35), there results

$$\rho = \sum_n \frac{V_n^i V_n^m}{1+j\lambda_n} \tag{1-37}$$

where V_n^m is the modal measurement coefficient

$$V_n^m = \langle J_n, E^m \rangle = \oiint_S \vec{J}_n \cdot \vec{E}^m ds \tag{1-38}$$

Note that V_n^m is of the same functional form as V_n^i, the excitation coefficient, given by (1-29). Hence, (1-37) is a symmetric bilinear functional of $\vec{E}^i$ (the impressed field, or excitation) and of $\vec{E}^m$ (the measurement field, or adjoint excitation). Of course, the symmetry of (1-37) is a consequence of the symmetry of the original operator Z.

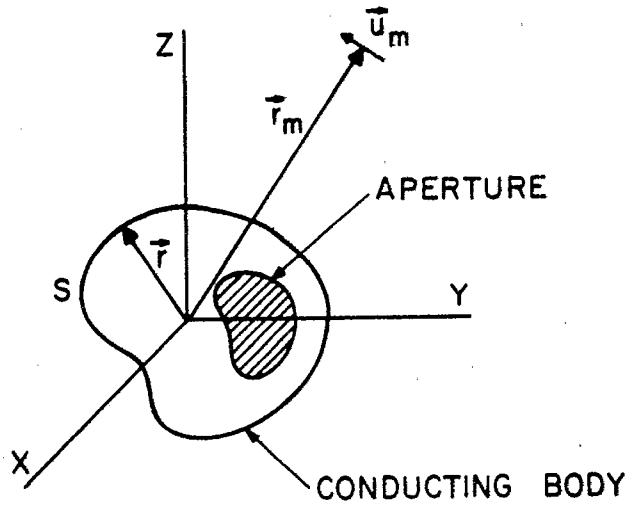

Fig. 1-2. An aperture antenna.

Reciprocal forms for the measurement coefficients, analogous to (1-33) and (1-34) for excitation coefficients, can also be written. For example, if the source of $\vec{E}^m$ is electric current $\vec{J}^m$, then

$$V_n^m = \iiint \vec{E}_n \cdot \vec{J}^m d\tau \tag{1-39}$$

analogous to (1-33). If the source of $\vec{E}^m$ is magnetic current $\vec{M}^m$, then

$$V_n^m = - \iiint \vec{H}_n \cdot \vec{M}^m d\tau \tag{1-40}$$

analogous to (1-34). Finally, if $\vec{E}^m$ is produced by both a $\vec{J}^m$ and an $\vec{M}^m$, the measurement coefficient V_n^m is given by the sum of (1-39) and (1-40).

VI. APPLICATION TO RADIATION AND SCATTERING PROBLEMS

Two important specializations of the general theory are (a) radiation from apertures in conducting bodies and (b) plane-wave scattering by conducting bodies. Explicit formulas for these two cases are given in this section. Other problems, such as antennas in the vicinity of conductors and near-field measurements, are also special cases of the general formulas, but they are not considered explicitly.

Consider a conducting body of surface S in which one or more apertures exist, as suggested by Figure 1-2. There are sources internal to S which produce a tangential electric field $\vec{E}_{tan}$ (assumed known) over the apertures. Then $\vec{E}^i = - \vec{E}_{tan}$ is the impressed field, and the mode excitation coefficients (1-29) become

$$V_n^i = - \oiint_S \vec{J}_n \cdot \vec{E}_{tan} ds \tag{1-41}$$

The radiation pattern for the aperture is then given by the modal solution (1-31). For computation, we must deal with one number at a time, say some component of $\vec{E}$ at a particular position (θ,ϕ) on S_∞. For this, we place a unit electric dipole $I\vec{\ell} = \vec{u}_m$ at (θ,ϕ) on S_∞, and evaluate the modal measurement coefficient by (1-38) and (1-39). This gives

$$V_n^m = \oiint_S \vec{J}_n \cdot \vec{E}^m ds = \vec{E}_n \cdot \vec{u}_m \tag{1-42}$$

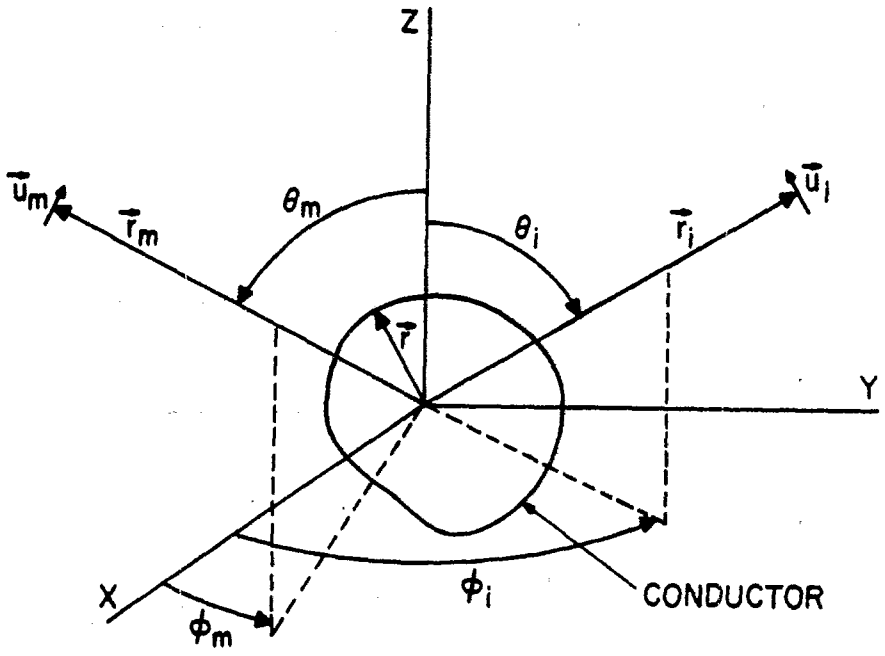

Fig. 1-3. A conducting scatterer.

where $\vec{E}^m$ is the field produced by the distant dipole. Explicitly, in the vicinity of S the dipole field is [5]

$$\vec{E}^m = \frac{-j\omega\mu}{4\pi r_m} e^{-jkr_m} (\vec{u}_m e^{-j\vec{k}_m \cdot \vec{r}}) \tag{1-43}$$

Here $\vec{k}_m$ is the vector propagation constant of the wave from $I\vec{\ell} = \vec{u}_m$, and $\vec{r}_m$ is the position vector to $I\vec{\ell}$ (see Figure 1-2). Now (1-42) becomes

$$V_n^m = \frac{-j\omega\mu}{4\pi r_m} e^{-jkr_m} \oiint_S \vec{J}_n \cdot \vec{u}_m e^{-j\vec{k}_m \cdot \vec{r}} ds \tag{1-44}$$

Substituting this into (1-31) dotted into $\vec{u}_m$, we have

$$\vec{E} \cdot \vec{u}_m = \frac{-j\omega\mu}{4\pi r_m} e^{-jkr_m} \sum_n \frac{V_n^i R_n^m}{1+j\lambda_n} \tag{1-45}$$

where V_n^i are given by (1-41) and

$$R_n^m = \oiint_S \vec{J}_n \cdot \vec{u}_m e^{-j\vec{k}_m \cdot \vec{r}} ds \tag{1-46}$$

are the plane-wave measurement coefficients. Equation (1-45) provides a convenient formula for computations.

Next, consider a conducting body of surface S in a plane-wave scattering problem, as suggested by Figure 1-3. The impressed field is the unit plane wave

$$\vec{E}^i = \vec{u}_i e^{-j\vec{k}_i \cdot \vec{r}} \tag{1-47}$$

where $\vec{u}_i$ is the polarization vector and $\vec{k}_i$ is the propagation vector. The excitation coefficients (1-29) are now

$$V_n^i = R_n^i = \oiint_S \vec{J}_n \cdot \vec{u}_i e^{-j\vec{k}_i \cdot \vec{r}} ds \tag{1-48}$$

Note that this is of the same functional form as the plane-wave measurement coefficients (1-46), hence the notation R_n^i for (1-48). The determination of the scattered field at some measurement position (θ_m, ϕ_m) is the same problem

as the determination of the radiation field in the antenna problem. Hence, the scattered field in the direction (θ_m,ϕ_m) is given by (1-45) with V_n^i replaced by R_n^i, or

$$\vec{E} \cdot \vec{u}_m = \frac{-j\omega\mu}{4\pi r_m} e^{-jkr_m} \sum_n \frac{R_n^i R_n^m}{1+j\lambda_n} \tag{1-49}$$

A commonly used parameter in plane-wave scattering problems is the echo area, defined as [5]

$$\sigma = 4\pi r_m^2 |\vec{E} \cdot \vec{u}_m|^2 \tag{1-50}$$

Substituting from (1-49) into (1-50), we obtain

$$\sigma = \frac{\omega^2\mu^2}{4\pi} \left| \sum_n \frac{R_n^i R_n^m}{1+j\lambda_n} \right|^2 \tag{1-51}$$

Note that σ is a function of the polarization of the incident wave $\vec{u}_i$, and of the measurement wave $\vec{u}_m$, as well as of the position coordinates (θ_i,ϕ_i) of the incident wave direction and (θ_m,ϕ_m) of the measurement direction.

VII. DYADIC REPRESENTATIONS

Any bilinear functional can be represented in terms of a dyadic operator, the Dirac bra-ket notation being well-suited for this purpose. In the modal solution for the current, let $E^i\rangle$ denote the tangential component of the impressed $\vec{E}$ on S, and $J\rangle$ a current on S. The characteristic currents are denoted by $J_n\rangle$ or $\langle J_n$. Then (1-30) becomes

$$J\rangle = \sum_n \frac{J_n\rangle\langle J_n, E^i\rangle}{1+j\lambda_n} \tag{1-52}$$

where we have used (1-29) for the excitation coefficients. Similarly, if $\langle E^m$ denotes the tangential component of the measurement field $\vec{E}^m$ on S, the general linear functional (1-37) becomes

$$\rho = \sum_n \frac{\langle E^m, J_n\rangle\langle J_n, E^i\rangle}{1+j\lambda_n} \tag{1-53}$$

where we have used (1-38) for the measurement coefficients. It is evident from (1-53) that

$$Y = Z^{-1} = \frac{J_n><J_n}{1+j\lambda_n} \tag{1-54}$$

is a dyadic representation for the inverse operator to Z, called the spectral form of $Y = Z^{-1}$. In terms of (1-54), we can write (1-52) as

$$J> = YE^i> \tag{1-55}$$

which is the inverse equation to our starting equation $ZJ> = E^i>$. Similarly, we can write (1-53) as

$$\rho = <E^m, YE^i> \tag{1-56}$$

The inverse to this equation is

$$\rho = <J^m, ZJ^i> \tag{1-57}$$

where $<J^m$ is the current on S excited by the measurement field $<E^m$, and $J^i>$ is the current on S excited by the impressed field $E^i>$.

If the impressed and measurement fields are produced by electric currents, we can use the reciprocal formulas (1-33) and (1-39) for the excitation and measurement coefficients. For this, we introduce the bilinear product

$$\{A,B\} = \iiint \vec{A} \cdot \vec{B}\, d\tau \tag{1-58}$$

where the integration is over all space. Now let $E\}$ denote the electric field $\vec{E}$ everywhere in space, and $J^i\}$ the impressed sources everywhere in space. In terms of the mode fields $E_n\}$ or $\{E_n$, we can now write the electric field (1-31) as

$$E\} = \sum_n \frac{E_n\}\ \{E_n,\ J^i\}}{1+j\lambda_n} \tag{1-59}$$

where we have used (1-33) for the excitation coefficients. Similarly, if $\{J^m$ denotes the source of the measurement field everywhere in space, the general linear functional (1-37) becomes

$$\rho = \sum_n \frac{\{J^m, E_n\}\{E_n, J^i\}}{1+j\lambda_n} \tag{1-60}$$

where we have used (1-39) for the measurement coefficients. It is now evident that

$$\Gamma = \sum_n \frac{E_n\}\{E_n}{1+j\lambda_n} \tag{1-61}$$

is a dyadic operator in spectral form. In terms of (1-61), we can write (1-59) as

$$E\} = \Gamma J^i\} \tag{1-62}$$

from which it is evident that Γ is a type of Green's function. Explicitly, it gives the field $\vec{E}$ due to $\vec{J}$ on S (sometimes called the scattered field) when the conducting body S is excited by impressed sources $\vec{J}^i$ elsewhere in space. Similarly, (1-60) can be written as

$$\rho = \{J^m, \Gamma J^i\} \tag{1-63}$$

which is an alternative form for the general bilinear functional ρ.

A development similar to the above applies for the $\vec{H}$ field if the impressed and measurement fields are produced by magnetic currents. To summarize, let $H_n\}$ or $\{H_n$ represent the magnetic modal fields, and define the magnetic dyadic operator

$$\hat{\Gamma} = \sum_n \frac{H_n\}\{H_n}{1+j\lambda_n} \tag{1-64}$$

Now, letting $M^i\}$ denote an impressed magnetic current, analogous to (1-59) and (1-62) we have

$$H\} = -\hat{\Gamma}M^i = -\sum_n \frac{H_n\}\{H_n, M^i\}}{1+j\lambda_n} \tag{1-65}$$

The minus sign is due to that appearing in (1-40). It is evident that $-\hat{\Gamma}$ is a magnetic Green's function, giving the field $\vec{H}$ due to $\vec{J}$ on S when the conducting body is excited by impressed sources $M^i\}$ elsewhere in space. Letting $\{M^m$ denote a measurement magnetic current, analogous to (1-60) and (1-63) we have

$$\rho = \{M^m, \hat{\Gamma} M^i\} = \sum_n \frac{\{M^m, H_n\}\{H_n, M^i\}}{1+j\lambda_n} \tag{1-66}$$

This is the most general form for a bilinear functional when both the impressed and measurement currents are magnetic.

If both electric and magnetic currents exist, it is convenient to use a six-component formulation for the problem [6]. In this case, field vectors $\psi = (\vec{E}, \vec{H})$ and source vectors $K = (\vec{J}, \vec{M})$ are defined, and equations (1-62) and (1-65) combined into a single six-component equation. We have no use at present for this generalization, and will not pursue it further.

Finally, if the electric currents for both the impressed and measurement sources are specialized to unit electric dipoles on the sphere at infinity, we obtain the bilinear scattering dyadic introduced by Garbacz [1,2]. To be explicit, let the unit incident plane wave be produced by the distant impressed dipole

$$I\vec{\ell}_i = \frac{-4\pi r}{j\omega\mu} e^{jkr} \vec{u}_i \tag{1-67}$$

and let the measurement source be the unit dipole $I\vec{\ell}_m = \vec{u}_m$. Let the ρ of (1-53) be $\vec{u}_m \cdot \vec{E}$, in which case (1-53) reduces to

$$\vec{u}_m \cdot \vec{E} = \frac{-4\pi r}{j\omega\mu} e^{jkr} \sum_n \frac{(\vec{u}_m \cdot \vec{E}_n)(\vec{E}_n \cdot \vec{u}_i)}{1+j\lambda_n} \tag{1-68}$$

The pattern functions $\vec{F}_n$ are defined by (1-21), and (1-68) can be written in terms of them as

$$\vec{u}_m \cdot \vec{E} = \frac{-j\omega\mu}{4\pi r} e^{-jkr} \sum_n \frac{(\vec{u}_m \cdot \vec{F}_n)(\vec{F}_n \cdot \vec{u}_i)}{1+j\lambda_n} \tag{1-69}$$

Defining the dyadic pattern operator as

$$\overleftrightarrow{F} = \sum_n \frac{\vec{F}_n \vec{F}_n}{1+j\lambda_n} \tag{1-70}$$

we can write (1-69) as

$$\vec{u}_m \cdot \vec{E} = \frac{-j\omega\mu}{4\pi r} e^{-jkr} (\vec{u}_m \cdot \overleftrightarrow{F} \cdot \vec{u}_i) \tag{1-71}$$

This is the $\vec{u}_m$ component of the scattered field due to a $\vec{u}_i$ polarized incident wave. The echo area, defined by (1-50), is given by

$$\sigma = \frac{(\omega\mu)^2}{4\pi} |\vec{u}_m \cdot \overleftrightarrow{F} \cdot \vec{u}_i|^2 \tag{1-72}$$

The dyadic operator $\overleftrightarrow{F}$ is valid only for the far field, not for the near field.

VIII. SCATTERING AND PERTURBATION MATRICES

The scattering matrix was first defined as that matrix which relates the amplitudes of incoming spherical modes to outgoing spherical modes [7]. More generally, the incoming and outgoing waves can be expanded in terms of arbitrary basis functions. We show that if the characteristic fields $\vec{E}_n$ are chosen as the basis of outgoing waves, and their conjugates $\vec{E}_n^*$ as the basis of incoming waves, then the scattering matrix is diagonalized.

In a scattering problem the far zone field can be expressed as the sum of incoming and outgoing waves as

$$\vec{E} = \vec{E}_{in} + \vec{E}_{out} \tag{1-73}$$

For a given scatterer, for each incoming wave $\vec{E}_{in}$ there is a unique outgoing wave $\vec{E}_{out}$. The scattering operator is defined to be that which operates on $\vec{E}_{in}$ to give $\vec{E}_{out}$, i.e.,

$$\vec{E}_{out} = S\,\vec{E}_{in} \tag{1-74}$$

Given an outgoing wave $\vec{E}_{out}$, the conjugate field $\vec{E}_{out}^*$ will be an incoming wave. This is evident from either spherical mode theory, or consideration of L^*, adjoint to L of (1-2). The characteristic fields $\vec{E}_n$ are outgoing waves, and we choose them as basis functions for $\vec{E}_{out}$, i.e.,

$$\vec{E}_{out} = \sum_n b_n \vec{E}_n \tag{1-75}$$

The conjugates $\vec{E}_n^*$ are incoming waves, and we choose them as basis functions for $\vec{E}_{in}$, i.e.,

$$\vec{E}_{in} = \sum_n a_n \vec{E}_n^* \tag{1-76}$$

The scattering matrix [S] is that which relates the column vector $\underline{b}$ (components b_n) to the column vector $\underline{a}$ (components a_n) according to

$$\underline{b} + [S]\,\underline{a} \tag{1-77}$$

A field of the form $\vec{E}_n + \vec{E}_n^*$ is a source-free field, shown as follows. The wave equation for the field $\vec{E}_n$ due to a current $\vec{J}_n$ is $\vec{\nabla} \times \vec{\nabla} \times \vec{E}_n + k^2\vec{E}_n = -j\omega\mu\vec{J}_n$. The field $\vec{E}_n^*$ satisfies the conjugate equation. Now if $\vec{J}_n$ is real, as it is for characteristic currents, then $\vec{E}_n + \vec{E}_n^*$ satisfies the source-free wave equation. Hence, in the absence of a body, the field will be a linear superposition of fields of the standing wave type $\vec{E}_n + \vec{E}_n^*$, i.e.,

$$\sum_n a_n(\vec{E}_n + \vec{E}_n^*) \tag{1-78}$$

It is evident from (1-75) to (1-78) that, when no body is present, $\underline{b} = \underline{a}$ and the scattering matrix is the identity matrix.

When a scatterer is present, the outgoing waves are partly due to the impressed field $\vec{E}^i$ and partly due to the field from the currents $\vec{J}$ on S, called the scattered field $\vec{E}^s$. The <u>perturbation operator</u> P is defined to be that which operates on $2\vec{E}_{in}$ to yield $\vec{E}^s$, i.e.,

$$\vec{E}^s = 2P\vec{E}_{in} \tag{1-79}$$

The factor 2 was introduced by Garbacz [1] for convenience in other formulas. The field $\vec{E}^s$ is an outgoing wave, and can be expanded in the $\vec{E}_n$ as

$$\vec{E}^s = \sum_n c_n \vec{E}_n \tag{1-80}$$

Expansion (1-76) is still used for $\vec{E}_{in}$. The perturbation matrix [P] is that which relates the column vector $\underline{c}$ (components c_n) to the column vector $\underline{a}$ according to

$$\underline{c} = 2[P]\,\underline{a} \tag{1-81}$$

It is evident from the definitions of [S] and [P] that

$$[S] = [I + 2P] \tag{1-82}$$

where [I] is the identity matrix.

We next show that both [S] and [P] are diagonal matrices, and obtain their elements. The impressed field $\vec{E}^i$ is a free-space field, and hence must be of the form (1-78). Because of linearity, it will suffice to show that a single-mode impressed field excites only the corresponding modal current. Hence, we assume an impressed field

$$\vec{E}^i = \vec{E}_m + \vec{E}_m^* \tag{1-83}$$

Then the mode excitation coefficients (1-29) are

$$V_n^i = \langle J_n, E_m + E_m^* \rangle = - \langle J_n, ZJ_m + Z^* J_m \rangle$$

$$= - (1+j\lambda_n + 1-j\lambda_n)\delta_{mn} = - 2\delta_{mn} \tag{1-84}$$

Thus, all mode coefficients are zero except V_m^i which is -2. From (1-31) we have

$$\vec{E}^s = \frac{-2\ \vec{E}_m}{1+j\lambda_m} \tag{1-85}$$

Hence, if $\vec{E}_{in}$ is $\vec{E}_m^*$, then $\vec{E}^s$ contains only $\vec{E}_m$ as shown by (1-85). If the incident field contains many modes as in (1-78), then the scattered field will contain a sum of terms of the form of (1-85). By comparison of (1-81) with (1-85), it is evident that

$$[P] = \begin{bmatrix} \frac{-1}{1+j\lambda_1} & 0 & 0 \ . \ . \ . \\ 0 & \frac{-1}{1+j\lambda_2} & 0 \ . \ . \ . \\ . \ . \ . \ . \ . \ . \ . \ . \ . \ . \ . \ . \ . \end{bmatrix} \tag{1-86}$$

i.e., [P] is diagonal with elements $-1/(1+j\lambda_n)$. Finally, from (1-82) we compute the scattering matrix as

$$[S] = \begin{bmatrix} \frac{1-j\lambda_1}{1+j\lambda_1} & 0 & 0 \ . \ . \ . \\ 0 & -\frac{1-j\lambda_2}{1+j\lambda_2} & 0 \ . \ . \ . \\ . \ . \ . \ . \ . \ . \ . \ . \ . \ . \ . \ . \ . \end{bmatrix} \tag{1-87}$$

i.e., [S] is diagonal with elements $-(1-j\lambda_n)/(1+j\lambda_n)$. These formulas agree with those of Garbacz [1].

IX. DISCUSSION

An extensive theory of the characteristic modes of conducting bodies is developed in this report, starting from the operator equation for the current on the body. These are the same modes obtained by Garbacz, who started from the scattering matrix. Our approach gives a simpler development of the theory than does Garbacz's, and we have derived a number of additional properties of the modes not discussed by Garbacz. The statement, made several times by Garbacz [1,4], that the perturbation operator transforms converging modes into diverging modes of the same form, is somewhat misleading. Our theory shows that the converging modes are transformed into diverging modes which are the complex conjugate of the converging modes. We have not considered the question of completeness of the sets of mode functions in Hilbert space. Garbacz [1] considers this question, and we find his arguments convincing.

The eigenvalues λ_n range from $-\infty$ to $+\infty$, with those of smallest magnitude being more important for radiation and scattering problems. We therefore order the modes according to $|\lambda_1| \leq |\lambda_2| \leq |\lambda_3| \leq \ldots$. Also, equation (1-24) shows that those modes with positive λ have predominantly stored magnetic energy, while those with negative λ have predominantly stored electric energy. We therefore call those modes with $\lambda > 0$ inductive modes, and those with $\lambda < 0$ capacitive modes. A mode having $\lambda = 0$ is called an externally resonant mode. The modes corresponding to the internal cavity resonances for the conducting surface have $|\lambda| = \infty$, and do not enter into radiation and scattering problems.

We concur with Garbacz's speculation that these modes should prove to be of great value, both theoretically and computationally, for radiation and scattering problems. In part 2 of this report we give a straightforward method for computing the modes. These computations bear out the speculation that, for electrically small and intermediate size bodies, only a few modes are needed to characterize the radiation and scattering properties of the conducting body. This property, coupled with the orthogonality properties of the modes, should make them valuable for synthesis and optimization problems in antenna and scattering theory.

PART 2

METHOD OF COMPUTATION

I. INTRODUCTION

A theory of characteristic modes for conducting bodies, which diagonalizes both the scattering operator and the impedance operator, is given in Part 1. A rather involved procedure for calculating the modes for wire objects was devised by Turpin [3], but because of computational difficulties he was able to obtain only four or five modes on a wire. Also, he gave no indication of how to extend his method to solid bodies. In this report we give a straightforward procedure for computing the modes on conducting bodies of arbitrary shape. The number of modes obtained is limited only by the speed and storage capabilities of the computer, not by inherent computational difficulties. Computer programs for conducting bodies of revolution and for wire objects will be given in future reports. We give illustrative computations of characteristic modes and of their use in radiation and scattering problems in this report.

II. BASIC EQUATIONS

The general theory is developed in Part 1 of this report. We here summarize some of the more important equations of this theory.

Given a surface S, let -L be the operator relating a current $\vec{J}$ on S to the electric field $\vec{E}$ it produces everywhere in space, i.e.,

$$L\vec{J} = -\vec{E} \tag{2-1}$$

Formulas for L in terms of vector and scalar potential integrals are given by (1-2) to (1-4). The impedance operator Z is given by L specialized to tangential components on the surface S, i.e.,

$$Z\vec{J} = (L\vec{J})_{tan} \tag{2-2}$$

Now Z is complex and symmetric, i.e., $Z = R + jX$ where its Hermitian components

$$R = \frac{1}{2}(Z + Z^*) \tag{2-3}$$

$$X = \frac{1}{2j}(Z - Z^*) \tag{2-4}$$

are real and symmetric. To diagonalize Z, we consider the weighted eigenvalue equation

$$Z\vec{J}_n = (1 + j\lambda_n) R\vec{J}_n \tag{2-5}$$

where $(1 + j\lambda_n)$ are eigenvalues and $\vec{J}_n$ are eigenfunctions. Substituting $Z = R + jX$ into (2-5), and cancelling the common terms, we obtain

$$X\vec{J}_n = \lambda_n R\vec{J}_n \tag{2-6}$$

This is a real symmetric eigenvalue equation, hence all eigenvalues λ_n are real and all eigenfunctions $\vec{J}_n$ are real. The $\vec{J}_n$ are called the characteristic currents of a conducting body S. The electric fields $\vec{E}_n$ produced by $\vec{J}_n$ according to (2-1) are called the characteristic fields of the conducting body S.

It is shown in Part 1 that the characteristic currents and fields have the following important properties:

(a) The characteristic currents are orthonormal over the surface S with weight R, i.e.,

$$\oiint_S \vec{J}_m \cdot R\vec{J}_n ds = \begin{cases} 0 & m \neq n \\ 1 & m = n \end{cases} \tag{2-7}$$

(b) The characteristic fields are orthonormal over the sphere at infinity S_∞ with weight $\sqrt{\varepsilon/\mu}$, i.e.,

$$\sqrt{\frac{\varepsilon}{\mu}} \oiint_{S_\infty} \vec{E}_m^* \cdot \vec{E}_n ds = \begin{cases} 0 & m \neq n \\ 1 & m = n \end{cases} \tag{2-8}$$

(c) The characteristic currents diagonalize the impedance operator for S. In particular, the current $\vec{J}$ on a conductor S in an impressed field $\vec{E}^i$ is given by

$$\vec{J} = \sum_n \frac{\vec{J}_n}{1+j\lambda_n} \oiint_S \vec{E}^i \cdot \vec{J}_n ds \tag{2-9}$$

(d) The characteristic fields diagonalize the scattering operator for S. More generally, the field $\vec{E}$ due to the current on a conductor S excited by impressed currents $\vec{J}^i$ is given by

$$\vec{E} = \sum_n \frac{\vec{E}_n}{1+j\lambda_n} \iiint \vec{E}_n \cdot \vec{J}^i d\tau \tag{2-10}$$

Here the integration extends over all space.

III. REDUCTION TO MATRIX EQUATIONS

The reduction of operator equations to matrix equations can be effected in the usual way by the method of moments [6]. For the space of square-integrable vector functions $\vec{A}$ and $\vec{B}$ on S we use the symmetric product

$$\langle A,B \rangle = \oiint_S \vec{A} \cdot \vec{B} \, ds \tag{2-11}$$

Because the mode currents are real, we use a set of real functions $\vec{W}_j$ as expansion functions for $\vec{J}_n$, i.e.,

$$\vec{J}_n = \sum_j I_j \vec{W}_j \tag{2-12}$$

where the I_j are coefficients to be determined. Substituting (2-12) into (2-6), and using the linearity of the operators, we obtain

$$\sum_j I_j X\vec{W}_j = \lambda_n \sum_j I_j R\vec{W}_j \tag{2-13}$$

To obtain symmetric matrices, we use the same $\vec{W}_i$ as testing functions. Taking the symmetric product of (2-13) with each $\vec{W}_i$, we have the set of equations

$$\sum_j I_j \langle W_i, XW_j \rangle = \lambda_n \sum_j I_j \langle W_i, RW_j \rangle \tag{2-14}$$

$i=1,2,\ldots$. This can be written as the matrix eigenvalue equation

$$[X][I]_n = \lambda_n [R][I]_n \tag{2-15}$$

where $[I]_n$ is the column matrix of the I_i, and

$$[R] = [\langle W_i, RW_j \rangle] \tag{2-16}$$

$$[X] = [\langle W_i, XW_j \rangle] \tag{2-17}$$

Equation (2-15) is a real, symmetric, weighted, matrix eigenvalue equation. Its eigenvalues λ_n approximate those of the operator equation (2-6), and its eigenvectors $[I]_n$ define functions according to (2-12) which approximate the eigenfunctions of (2-6).

The corresponding matrix approximation to the complex eigenvalue equation (2-5) is

$$[Z][I]_n = (1 \mp j\lambda_n)[R][I]_n \tag{2-18}$$

where $[Z] = [R + jX]$. The matrix $[Z]$ is known as the generalized impedance of the body [6], and has been evaluated in a number of cases [8,9]. If the $\vec{W}_i$ are differentiable, a convenient formula for the impedance elements is [8]

$$Z_{ij} = \oiint_S ds' \oiint_S ds[j\omega\mu\vec{W}_i' \cdot \vec{W}_j + \frac{1}{j\omega\varepsilon}(\vec{\nabla}' \cdot \vec{W}_i')(\vec{\nabla} \cdot \vec{W}_j)]\psi_Z \tag{2-19}$$

where the primes denote functions of the primed coordinates, and

$$\psi_Z = \frac{e^{-jk|\vec{r} - \vec{r}'|}}{4\pi|\vec{r} - \vec{r}'|} \tag{2-20}$$

The Hermitian parts of $[Z]$ are its real part $[R]$ and its imaginary part $[X]$, obtained in the conventional way. In particular, the elements R_{ij} are given by (2-19) with ψ_Z replaced by

$$\psi_R = \frac{\sin k|\vec{r} - \vec{r}'|}{j4\pi|\vec{r} - \vec{r}'|} \tag{2-21}$$

and the elements X_{ij} are given by (2-19) with ψ_Z replaced by

$$\psi_X = \frac{\cos k|\vec{r} - \vec{r}'|}{4\pi|\vec{r} - \vec{r}'|} \tag{2-22}$$

Numerical evaluation of these elements is considered in the literature [8,9].

The matrix equivalents of the orthogonality relationships for the characteristic currents, equations (1-16), are also of interest. For example, that for R is

$$\langle J_m, RJ_n \rangle = \langle \sum_i I_{i,m} W_i, R \sum_j I_{j,n} W_j \rangle$$

$$= \sum_{i,j} I_{i,m} I_{j,n} \langle W_i, RW_j \rangle$$

$$= [\tilde{I}]_m [R][I]_n = \delta_{mn} \qquad (2\text{-}23)$$

where ~ denotes transpose. Similar derivations hold for X and Z, giving the orthogonality relationships.

$$[\tilde{I}]_m [R][I]_n = \delta_{mn}$$

$$[\tilde{I}]_m [X][I]_n = \lambda_n \delta_{mn} \qquad (2\text{-}24)$$

$$[\tilde{I}]_m [Z][I]_n = (1+j\lambda_n)\delta_{mn}$$

Because the $[I]_m$ are real, these orthogonality relationships also apply with transposes replaced by transpose conjugates (Hermitian transpose).

IV. EVALUATION OF THE MODES

We next discuss solution of the matrix eigenvalue equation

$$[X][I] = \lambda[R][I] \qquad (2\text{-}25)$$

which is (2-15) with the subscript n dropped for brevity. The conventional method for reducing (2-25) to a symmetric unweighted eigenvalue equation requires [R] to be positive definite [10]. In our problem [R] is positive semidefinite in theory, but because of numerical inaccuracies it is actually indefinite, with some small negative eigenvalues. We therefore modify the conventional method as follows.

Let [U] be the orthogonal matrix which diagonalizes R according to

$$[\mu] = [\tilde{U}\ R\ U] = \begin{bmatrix} \mu_1 & 0 & 0 \ldots \\ 0 & \mu_2 & 0 \ldots \\ \ldots & \ldots & \ldots \end{bmatrix} \tag{2-26}$$

where the μ_i are the eigenvalues of R ordered $\mu_1 \geq \mu_2 \geq \ldots$. Premultiplying (2-25) by $[\tilde{U}]$, and using (2-26), we obtain

$$[\tilde{U}\ X\ U][\tilde{U}\ I] = \lambda[\mu][\tilde{U}\ I] \tag{2-27}$$

Only the larger μ_i can be considered accurate, and we set all $\mu_i < M\mu_1$ equal to zero, where M is some small number set by our estimated accuracy of [R]. (We usually take $M = 10^{-3}$.) The diagonal matrix $[\mu]$ is then partitioned as

$$[\mu] = \begin{bmatrix} [\mu_{11}] & [0] \\ [\ 0\ ] & [0] \end{bmatrix} \tag{2-28}$$

where $[\mu_{11}]$ contains all μ_i not considered zero. We also partition the other matrices in (2-27) conformably with $[\mu]$, i.e.,

$$[x] = [\tilde{U}\ I] = \begin{bmatrix} [x_1] \\ [x_2] \end{bmatrix} \tag{2-29}$$

$$[A] = [\tilde{U}\ X\ U] = \begin{bmatrix} [A_{11}] & [A_{12}] \\ [\tilde{A}_{12}] & [A_{22}] \end{bmatrix} \tag{2-30}$$

Substituting (2-28), (2-29), and (2-30) into (2-27), we obtain the two matrix equations

$$[A_{11}][x_1] + [A_{12}][x_2] = \lambda[\mu_{11}][x_1] \tag{2-31}$$

$$[\tilde{A}_{12}][x_1] + [A_{22}][x_2] = 0 \tag{2-32}$$

The second of these may be solved for $[x_2]$, and the result substituted into the first to obtain

$$[A_{11} - A_{12}A_{22}^{-1}\tilde{A}_{12}][x_1] = \lambda[\mu_{11}][x_1] \tag{2-33}$$

Now $[\mu_{11}]$ has only positive diagonal elements, and we can define the real matrix

$$[\mu_{11}^{1/2}] = \begin{bmatrix} \sqrt{\mu_1} & 0 & 0 \ldots \\ 0 & \sqrt{\mu_2} & 0 \ldots \\ \ldots\ldots\ldots\ldots \end{bmatrix} \tag{2-34}$$

Substituting $[\mu_{11}] = [\mu_{11}^{1/2}][\mu_{11}^{1/2}]$ into (2-33), and multiplying by $[\mu_{11}^{-1/2}]$, we obtain

$$[\mu^{-1/2}][A_{11} - A_{12}A_{22}^{-1}\tilde{A}_{12}][\mu_{11}^{-1/2}][\mu_{11}^{1/2}x_1] = \lambda[\mu_{11}^{1/2}x_1] \tag{2-35}$$

This is now the real, symmetric, unweighted eigenvalue equation

$$[B][y] = \lambda[y] \tag{2-36}$$

where the definition of [B] and [y] is obvious by comparing (2-36) with (2-35). The eigenvalues of (2-36) are the smaller eigenvalues of our original equation (2-25), and the eigenvectors of (2-36) give the corresponding eigenvectors of (2-25) according to

$$[I] = [Ux] = [U]\begin{bmatrix} [\delta] \\ [-A_{22}^{-1}\tilde{A}_{12}] \end{bmatrix}[\mu_{11}^{-1/2}y] \tag{2-37}$$

where $[\delta]$ is the identity matrix.

To diagonalize the real symmetric matrices [R] and [B] we used the Jacobi method [11], available in the IBM System/360 scientific subroutine package (EIGEN). We have also used the Givens-Householder method [11], but the accuracy of the dominant λ, as checked by the Rayleigh quotient, was not as good as for the Jacobi method. Other methods tried were solution of $[R^{-1}X][I] = \lambda[I]$ and $(1/\lambda)[I] = [X^{-1}R][I]$ by the QR double step method [12], but again the accuracy was not as good as for the Jacobi method. Also, as a numerical check, we used the Gram-Schmidt procedure to calculate a set of orthogonal eigenvectors corresponding to $\mu_i = 0$. The complete set of eigenvectors $[I]_n$ was orthogonal to within the accuracy of computation.

Finally, the characteristic currents $\vec{J}_n$ are given by (2-12), where I_i are the components of $[I]_n$, and the characteristic fields are given by

$$\vec{E}_n = - L\vec{J}_n = - \sum_i I_i L\vec{W}_i \tag{2-38}$$

However, rather than evaluate $L\vec{W}_i$ numerically, we use reciprocity as discussed in Section VI of Part 1. For this, we place the unit current element $I\vec{\ell} = \vec{u}_m$ at the point of measurement, and compute the m-th component of $\vec{E}_n$ as

$$\vec{E}_n \cdot \vec{u}_m = \oiint_S \vec{E}^m \cdot \vec{J}_n ds$$

$$= \sum_i I_i \oiint_S \vec{E}^m \cdot \vec{W}_i ds \tag{2-39}$$

The final integrals are measurement coefficients with respect to the $\vec{W}_i$. If the radiation pattern is desired, we place $\vec{u}_m$ on the sphere at infinity and compute the m-th component of the radiation field as

$$\vec{E}_n \cdot \vec{u}_m = \frac{-j\omega\mu}{4\pi r_m} e^{-jkr_m} \sum_i I_i R_i \tag{2-40}$$

where R_i are the plane-wave measurement coefficients

$$R_i = \oiint_S \vec{W}_i \cdot \vec{u}_m e^{-j\vec{k}_m \cdot \vec{r}} ds \tag{2-41}$$

The notation of (2-40) and (2-41) is discussed in Section VI of Part 1.

V. APPLICATION TO BODIES OF REVOLUTION

A general computer program for calculating the characteristic modes on conducting bodies of revolution has been developed and will be published in the future. An outline of this program and some illustrative examples of its use are given here.

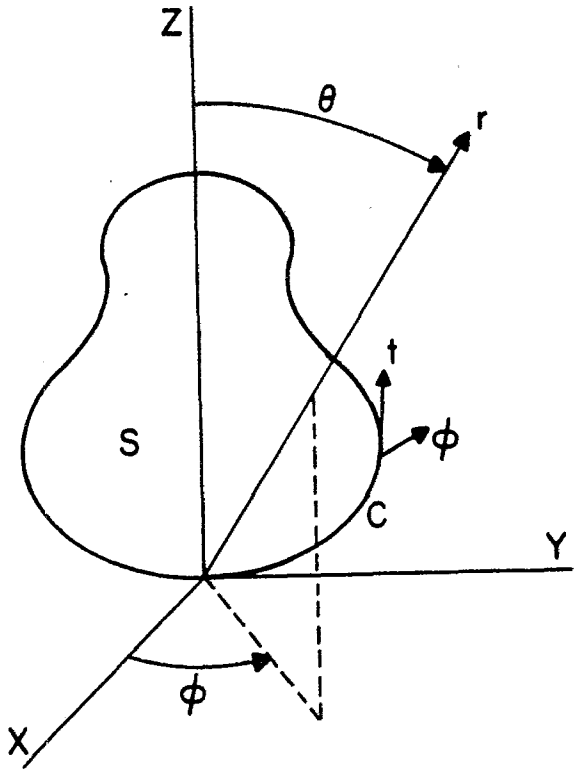

Fig. 2-1. Coordinate system for bodies of revolution.

Figure 2-1 defines the coordinate system used for bodies of revolution. The body S is generated by rotating the contour C about the z axis. The coordinates on S are t (length variable along C) and ϕ (angle of rotation from the x-axis). The spherical coordinates of a field point are r,θ,ϕ. The current $\vec{J}$ on S has two components, J_t and J_ϕ. Letting $\vec{u}_t$ and $\vec{u}_\phi$ denote unit vectors in the t and ϕ directions, we can choose two sets of real expansion functions

$$\{\vec{u}_t f_i(t),\ \vec{u}_t f_i(t) \cos n\phi,\ \vec{u}_\phi f_i(t) \sin n\phi\} \tag{2-42}$$

and

$$\{u_\phi f_i(t),\ \vec{u}_t f_i(t) \sin n\phi,\ -\vec{u}_\phi f_i(t) \cos n\phi\} \tag{2-43}$$

where i and n are positive integers. These two sets are sufficiently general to represent an arbitrary $\vec{J}$ on S if the $f_i(t)$ form a complete set in the t domain. If the testing function $\vec{W}_i'$ is from the set (2-42), and the expansion function $\vec{W}_j$ is from the set (2-43), then the resulting impedance element (2-19) is zero. The sets (2-42) and (2-43) can therefore be treated independently. The impedance matrix for the set (2-42) has the block diagonal form

$$[Z] = \begin{bmatrix} [Z_0^{tt}] & [0] & [0] \ldots \\ [0] & [Z_1] & [0] \ldots \\ [0] & [0] & [Z_2] \\ \ldots\ldots\ldots\ldots\ldots \end{bmatrix} \tag{2-44}$$

where, for n=1,2,...,

$$[Z_n] = \begin{bmatrix} [Z_n^{tt}] & [Z_n^{t\phi}] \\ [Z_n^{\phi t}] & [Z_n^{\phi\phi}] \end{bmatrix} \tag{2-45}$$

The submatrices on the right-hand side of (2-45) are computed using the following expansion and testing functions:

Table 1

Matrix element	Testing function	Expansion function
$(Z_n^{tt})_{ij}$	$\vec{u}_t f_i(t) \cos n\phi$	$\vec{u}_t f_j(t) \cos n\phi$
$(Z_n^{t\phi})_{ij}$	$\vec{u}_t f_i(t) \cos n\phi$	$\vec{u}_\phi f_j(t) \sin n\phi$
$(Z_n^{\phi t})_{ij}$	$\vec{u}_\phi f_i(t) \sin n\phi$	$\vec{u}_t f_j(t) \cos n\phi$
$(Z_n^{\phi\phi})_{ij}$	$\vec{u}_\phi f_i(t) \sin n\phi$	$\vec{u}_\phi f_j(t) \sin n\phi$

The orthogonality between sets (2-42) and (2-43), as well as the block diagonal form of (2-44), is a consequence of equations (33) to (37) of reference [8]. This is equivalent to the statement that a current of the form $\vec{J} = \vec{u}_t J_t \cos n\phi + \vec{u}_\phi J_\phi \sin n\phi$ produces a tangential electric field on S of the same form, $\vec{E}_{tan} = \vec{u}_t E_t \cos n\phi + \vec{u}_\phi E_\phi \sin n\phi$, and that a current of the form $\vec{J} = \vec{u}_t J_t \sin n\phi - \vec{u}_\phi J_\phi \cos n\phi$ produces a tangential electric field on S of the same form, $\vec{E}_{tan} = \vec{u}_t E_t \sin n\phi - \vec{u}_\phi E_\phi \cos n\phi$.

The impedance elements can now be evaluated in terms of those used in earlier work [8]. Letting the careted matrices denote those of equation (39) of reference [8], we obtain

$$[Z_o^{tt}] = [\hat{Z}_o^{tt}] \tag{2-46}$$

$$[Z_n] = \frac{1}{2}\begin{bmatrix} [\hat{Z}_n^{tt}] & -j[\hat{Z}^{t\phi}] \\ j[\hat{Z}_n^{\phi t}] & [\hat{Z}_n^{\phi\phi}] \end{bmatrix} \tag{2-47}$$

This result is obtained by expressing sin $n\phi$ and cos $n\phi$ in terms of exponentials. For example, the elements of $[Z_n^{t\phi}]$ are given by

$$(Z_n^{t\phi})_{ij} = \langle \vec{u}_t f_i(t) \cos n\phi, \; Z\vec{u}_\phi f_j(t) \sin n\phi \rangle$$

$$= \frac{1}{4j} (\hat{Z}_n^{t\phi})_{ij} - \frac{1}{4j} (\hat{Z}_{-n}^{t\phi})_{ij}$$

$$= \frac{1}{2j} (\hat{Z}_n^{t\phi})_{ij} \qquad (2\text{-}48)$$

Similar derivations yield the other submatrices of (2-47).

The impedance matrix for the set (2-43) has the same form as (2-44) except that $[Z_o^{tt}]$ is replaced by $[Z_o^{\phi\phi}]$. The table of expansion and testing functions must now be changed by replacing all cos $n\phi$ factors by sin $n\phi$ factors, and all sin $n\phi$ factors by -cos $n\phi$ factors. The relationship of these new impedance matrices to those of [8] is now given by

$$[Z_o^{\phi\phi}] = [\hat{Z}_o^{\phi\phi}] \qquad (2\text{-}49)$$

and by (2-47) for $n > 0$.

For computation, we specify 2N+1 nearly equidistant points $t_0, t_1, \ldots, t_{2N}$ along C, with t_0 at the beginning and t_{2N} at the end of C. The $f_i(t)$ are taken as triangle functions divided by the radius, each extending over four intervals $(t_j - t_{j-1})$. For expansion, the $f_i(t)$ are approximated by four pulses, and for testing they are approximated by four impulses. The details are given in reference [8]. Because of these approximations, the impedance matrices are not exactly symmetric, as they would be if evaluated exactly. We eliminated this asymmetry by averaging corresponding off diagonal elements of [Z]. A number of computational checks showed that this averaging had no noticeable affect in radiation and scattering problems.

The computer program for bodies of revolution was first run for spherical conductors, and the results compared to the exact modal solution. Table 2 shows a comparison of the exact λ (computed from spherical mode theory) to the approximate λ (computed from our general program) for a few of the modes. The computations are for a sphere of radius 0.2 wavelength using 9 expansion functions for J_t and 9 for J_ϕ (the [Z] is 18 by 18). These numbers are smaller than usually used. Sources of error in the computations are (a) the circular contour is approximated by 20 straight line segments, (b) the current is

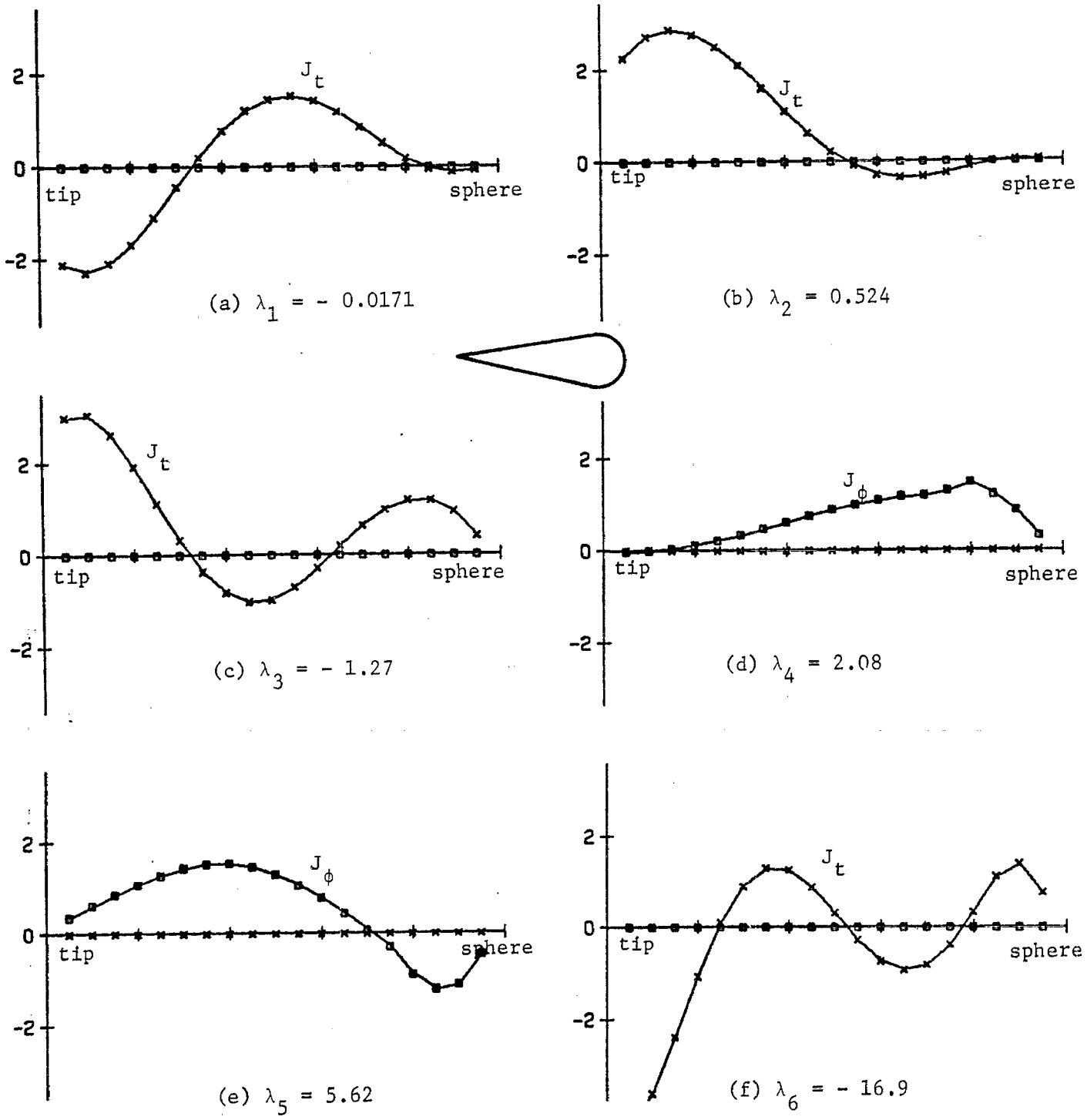

Fig. 2-2. Characteristic currents for a cone-sphere, length 1.36 wavelengths, sphere diameter 0.4 wavelengths. The six lowest order rotationally symmetric modes are shown.

approximated by triangle functions divided by radius, and (c) approximations are introduced into the evaluation of [Z]. The accuracy of the approximate λ decreases as the exact $|\lambda|$ gets larger, but such modes are less important in radiation and scattering problems. The accuracy of computation increases as the number of contour segments is increased. Plots of some of the approximate mode currents, compared to the exact mode currents, are given in Appendix B.

Table 2. Comparison of exact λ and approximate λ for a sphere of radius 0.2 wavelength.

Mode	Exact λ	Approx. λ
TE_{01}	2.673	2.682
TE_{02}	21.60	21.82
TM_{01}	-1.082	-1.096
TM_{03}	-284.4	-290.7
TE_{12}	21.60	21.66
TM_{12}	-11.00	-11.30
TE_{22}	21.60	21.56
TM_{22}	-11.00	-11.26

The general program was next run for a number of bodies of revolution with contours of different shapes. For representative computations, consider a cone-sphere body, formed by a cone of 10° half-angle smoothly joined to a sphere of diameter 0.4 wavelength (approximate total length 1.36 wavelengths). The contour is approximated by 40 straight-line segments of equal length, and 19 expansion functions are used for J_t and J_ϕ (the [Z] is 38 by 38). Figure 2-2 shows the six lowest order characteristic currents for the rotationally symmetric modes (n=0), plotted vs. the contour length variable, starting at the tip and ending on the sphere. These modes are the ones which are used in the solution of radiation from rotationally symmetric apertures. The x's denote t-directed currents, and the squares denote ϕ-directed currents. In the rotationally symmetric case, if J_t is nonzero, then $J_\phi = 0$, and vice versa.

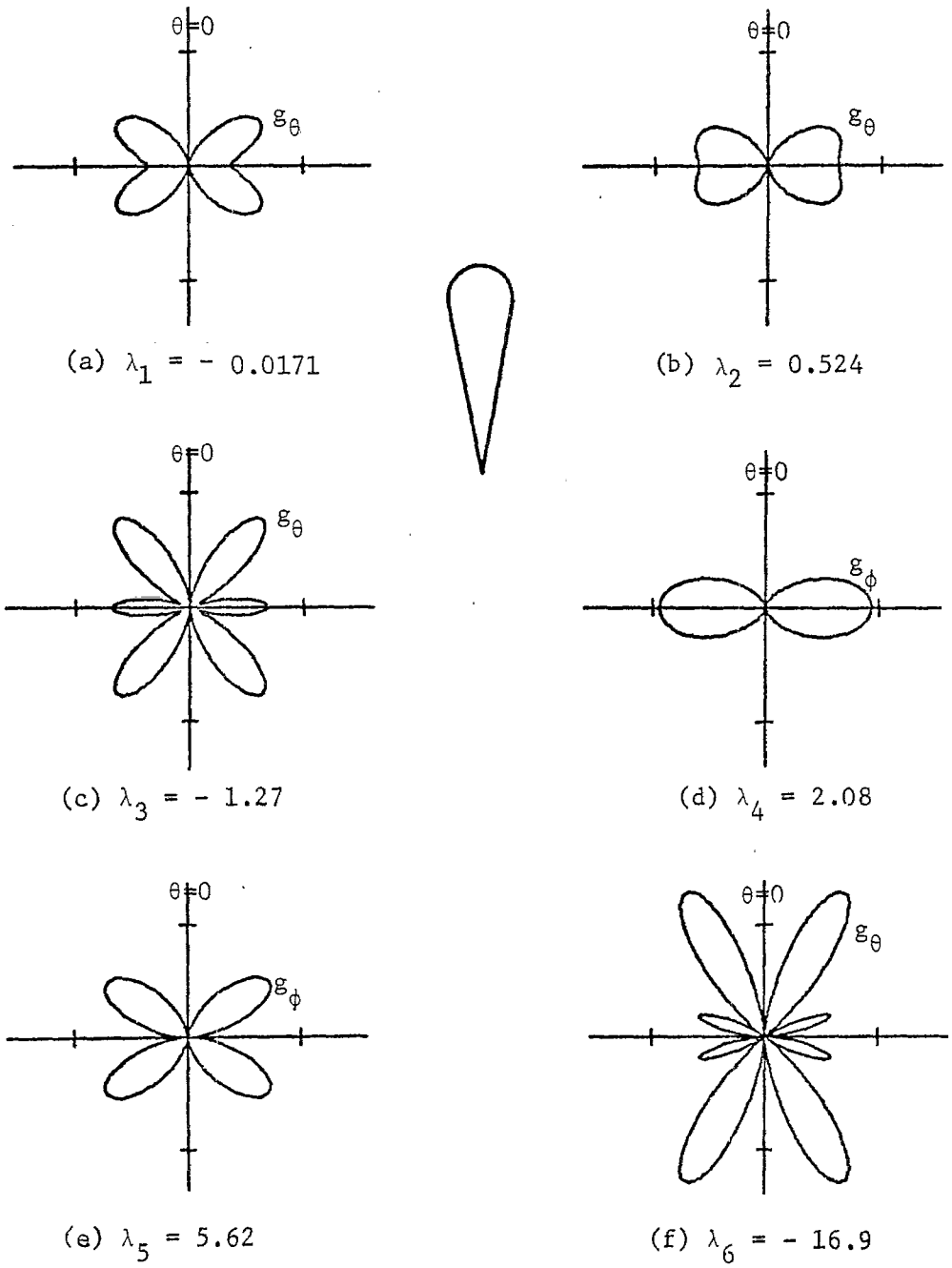

Fig. 2-3. Characteristic gain patterns for a cone-sphere, length 1.36 wavelengths, sphere diameter 0.4 wavelengths. The six lowest order rotationally symmetric modes are shown.

Note that the first three modes have only J_t, and are similar to straight wire modes. The next two modes have only J_ϕ, and are similar to wire loop modes. The value of λ in each case is listed under the corresponding graph. The currents are normalized so that their mean-square value over the surface is unity.

Figure 2-3 shows the characteristic gain patterns for the six lowest order rotationally symmetric modes of the cone-sphere. They are plots of the normalized radiation intensity vs. θ from the corresponding mode currents of Figure 2-2. (Tic marks correspond to a gain of 2.) The first three modes are due to J_t, and have only an E_θ in the radiation field. The next two modes are due to J_ϕ, and have only an E_ϕ in the radiation field. The three-dimensional pattern is obtained by rotating each plot about the Z axis (vertical axis).

Figure 2-4 shows the six lowest order characteristic currents for the cos ϕ, sin ϕ modes (n=1) of the same cone-sphere. These are the modes which are used in the solution of scattering due to a plane-wave axially incident on the body. Now each mode has both a J_t (plotted by x's) and a J_ϕ (plotted by squares), where J_t varies as cos ϕ and J_ϕ varies as sin ϕ. The graphs are for J_t in the $\phi = 0$ plane, and J_ϕ in the $\phi = \pi/2$ plane. The small oscillations in J_ϕ are due to inaccuracies of computation. The true J_ϕ is probably that obtained by smoothing out the oscillations. Again the currents are normalized so that their mean-square value over the surface is unity.

Figure 2-5 shows the characteristic gain patterns for the six lowest order cos ϕ, sin ϕ modes of the cone-sphere. They are plots of the normalized radiation intensity vs. θ from the corresponding mode currents of Figure 2-4. (Again, tic marks correspond to a gain of 2.) Now the radiation field for each mode has two components, E_θ which varies as cos ϕ, and E_ϕ which varies as sin ϕ. The graph labeled g_θ is the θ-polarized gain in the $\phi = 0$ plane, and that labeled g_ϕ is the ϕ-polarized gain in the $\phi = \pi/2$ plane.

To illustrate computations for a body of another shape, Figure 2-6 shows similar results for a disk of one wavelength diameter. Shown are the three lowest order characteristic currents and characteristic gain patterns for the cos ϕ, sin ϕ (n=1) modes. The interpretation of the two components of J, and

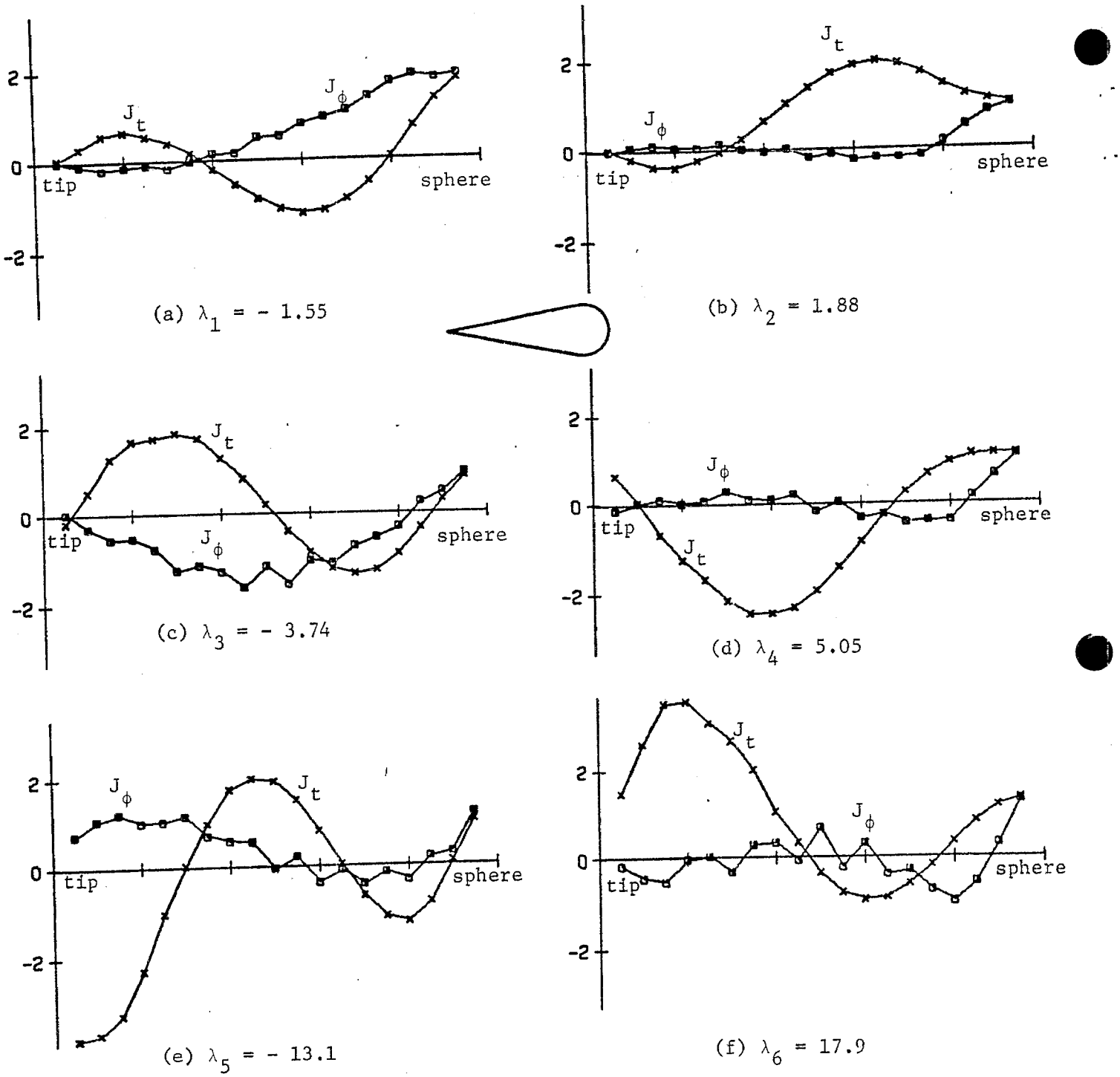

Fig. 2-4. Characteristic currents for a cone-sphere, length 1.36 wavelengths, sphere diameter 0.4 wavelengths. The six lowest order sin ϕ, cos ϕ modes are shown.

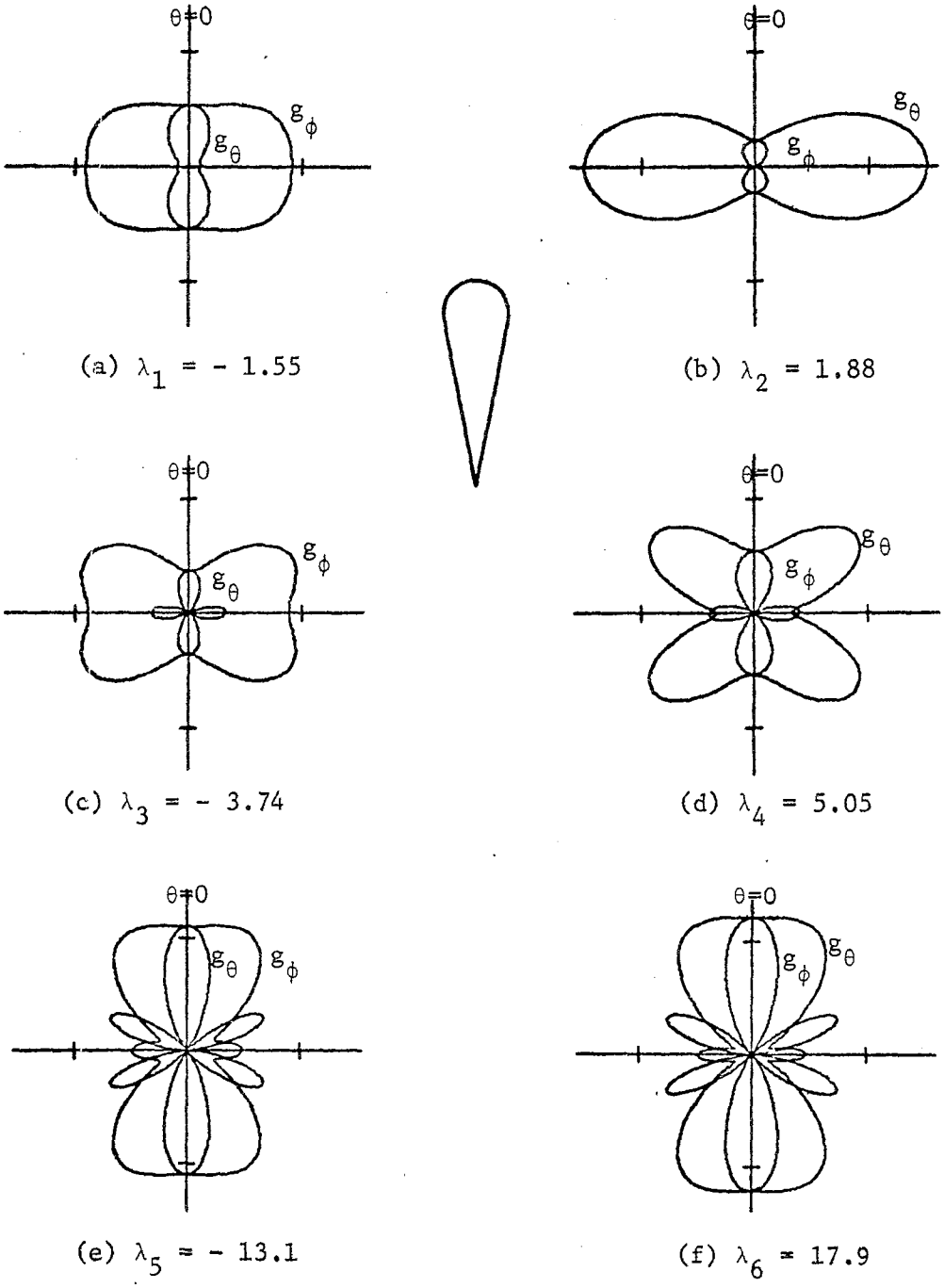

Fig. 2-5. Characteristic gain patterns for a cone-sphere, length 1.36 wavelengths, sphere diameter 0.4 wavelengths. The six lowest order sin ϕ, cos ϕ modes are shown.

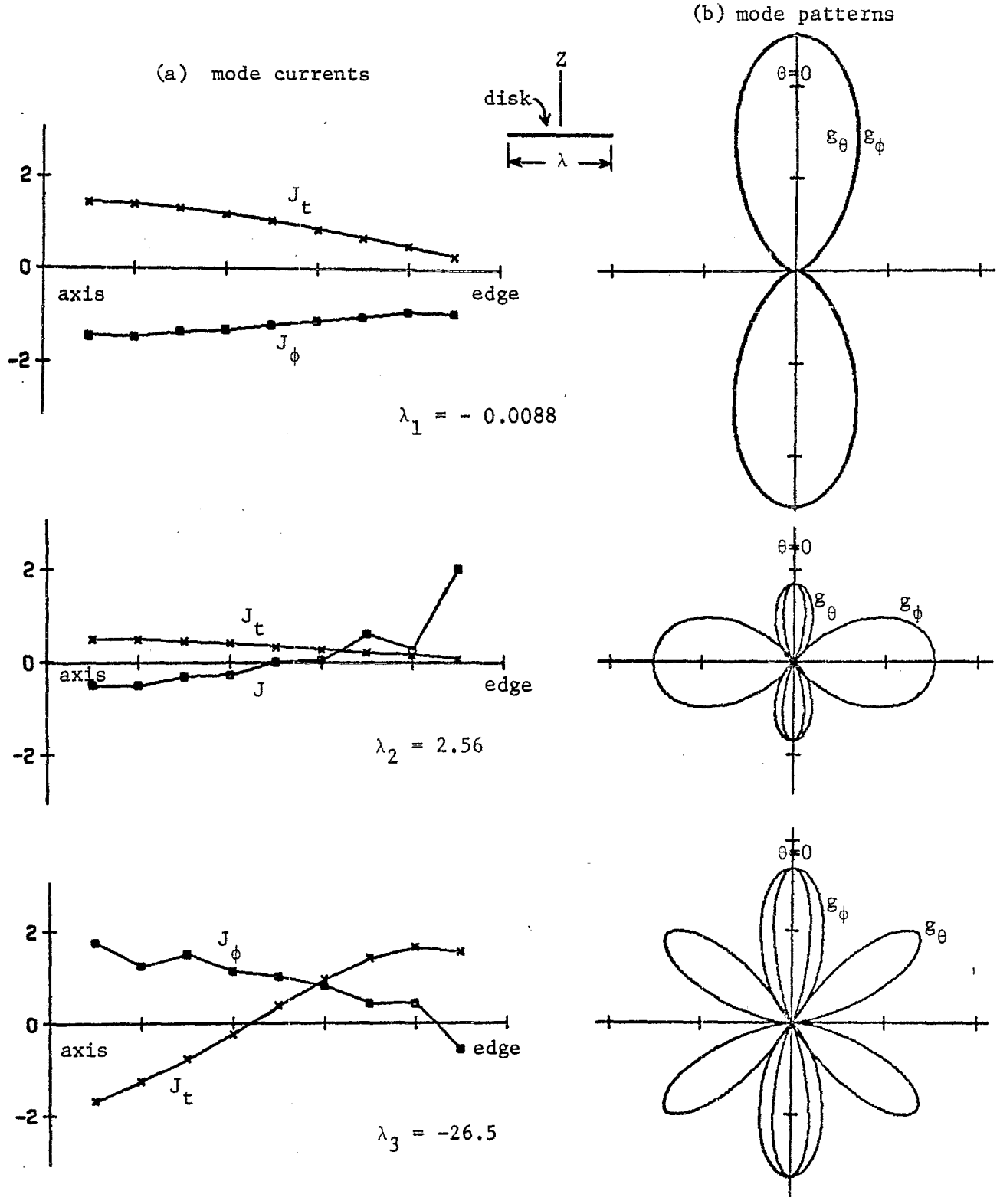

Fig. 2-6. Characteristic currents and gain patterns for a disk of one wavelength diameter. The three lowest order sin ϕ, cos ϕ modes are shown.

the two components of g, is the same as discussed for the cone-sphere.. The computations were made using 9 expansion functions for J_t and 9 for J_ϕ (an 18 by 18 matrix). Note that the lowest order mode is almost resonant, that is, its λ is almost zero.

VI. CONVERGENCE OF RADIATION AND SCATTERING PATTERNS

We have implied that only a few modes are needed to characterize the radiation and scattering properties of electrically small and intermediate size bodies. We now demonstrate that this is indeed true by computing the modal solutions for varying numbers of modes, and showing that their radiation and scattering patterns rapidly converge to known solutions.

The general theory of modal solutions is given in Section VI of Part 1. For aperture radiation problems, we use (1-12) in (1-41) to obtain the mode excitation coefficients as

$$V_n^i = - \sum_i I_i \oiint_S \vec{W}_i \cdot \vec{E}_{tan} ds \tag{2-50}$$

where $\vec{E}_{tan}$ is the assumed tangential $\vec{E}$ over S. Similarly, we evaluate the plane-wave measurement coefficients (1-46) as

$$R_n^m = \sum_i I_i \oiint_S \vec{W}_i \cdot \vec{u}_m \, e^{-j\vec{k}_m \cdot \vec{r}} ds \tag{2-51}$$

where $\vec{u}_m$ and $\vec{k}_m$ are the polarization and propagation vectors, respectively, of the measurement plane wave. In evaluating (2-50) and (2-51) for bodies of revolution, we use a four impulse approximation to $\vec{W}_i$, as discussed in reference [8]. Once V_n^i and R_n^m are evaluated, the radiation field is given by (1-45). For plane-wave scattering problems, we evaluate the plane-wave excitation coefficients R_n^i, equation (1-48), by (2-51) with $\vec{u}_m$ and $\vec{k}_m$ replaced by $\vec{u}_i$ and $\vec{k}_i$, the polarization and propagation vectors of the incident plane wave. Once R_n^i and R_n^m are evaluated, the bistatic radar cross section is given by (1-51).

Figure 2-7 illustrates convergence of the modal solution for the cone sphere (10° half cone angle, 0.2 wavelength sphere radius, 1.36 wavelengths

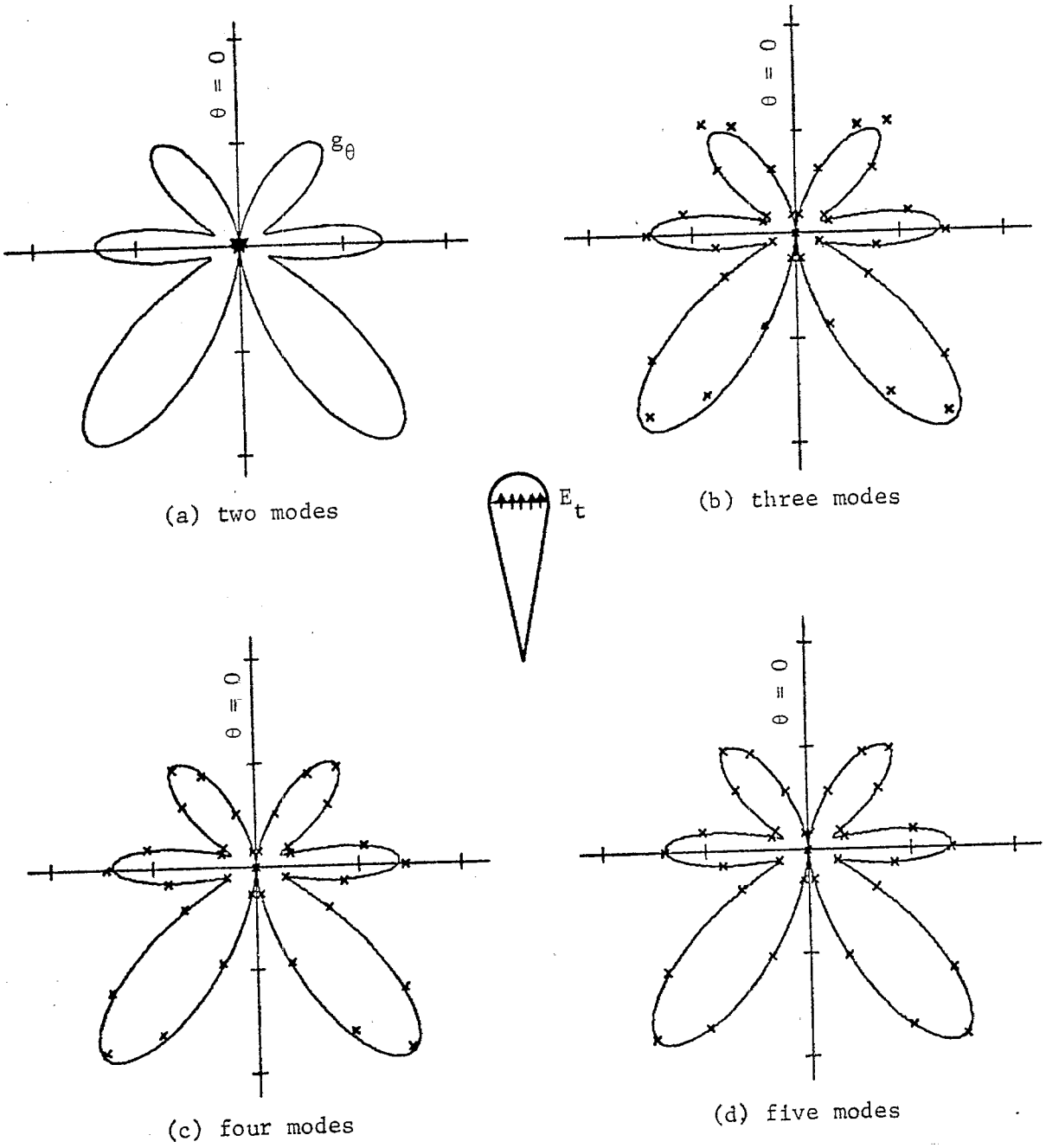

Fig. 2-7. Convergence of the modal solution for the cone-sphere excited by a voltage across a slot at the cone-to-sphere junction. Solid curves are the matrix inversion solution, x's are the modal solutions.

total length) excited by a voltage applied across a narrow slot at the cone-to-sphere junction. The solid curve in each figure is the radiation gain pattern obtained by matrix inversion [8], and the x's are the corresponding modal solution. The modes used are the rotationally symmetric ones having only J_t on S (Figure 2-2) and E_θ in the radiation field (Figure 2-3). These are the only ones which are excited by an E_t on S. The modal solution of Figure 2-7a uses the two lowest order modes, and is nearly zero. This could have been predicted from the fact that the two lowest characteristic currents, Figure 2-2a and b, have almost zero amplitude at the cone-to-sphere junction. The modal solution of Figure 2-7b uses the three lowest order modes, and shows that the gain pattern is predominantly that of the third mode. The modal solution of Figure 2-7c uses the four lowest order J_t modes, and that of 2-7d uses the five lowest order J_t modes. Note that the gain pattern is essentially fully converged when five modes are used.

Figure 2-8 illustrates convergence of the modal solution for the same cone-sphere scattering an x-polarized plane wave axially incident on the cone tip. The solid curves in each figure are the bistatic radar cross sections (E-plane and H-plane) obtained by matrix inversion [8]. The x's in each figure are the modal E-plane solution (θ-polarized, $\phi = 0$ plane), and the squares are the modal H-plane solution (ϕ-polarized, $\phi = \pi/2$ plane). The modes used are the $\cos \phi$, $\sin \phi$ (n=1) modes of Figures 2-4 and 2-5. The modal solution of Figure 2-8a uses the two lowest order modes, 2-8b the four lowest, 2-8c the six lowest, and 2-8d the eight lowest. Note that a plane wave excites all n=1 modes, the six lowest order modes being most important for this particular body. The scattering pattern has fully converged when eight modes are used.

We have also considered the convergence of modal solutions for bodies of other shape, with similar results. For example, for the disk of one wavelength diameter (characteristic currents and patterns given by Figure 2-6), the modal plane-wave scattering pattern was almost the same as that of the lowest order mode, which was resonant. The scattering pattern using two modes was almost identical to the matrix inversion solution.

If a conducting body of revolution is excited by a non-axially propagating plane wave, the n=0 modes, n=1 modes and higher order $\sin n\phi$, $\cos n\phi$ modes are

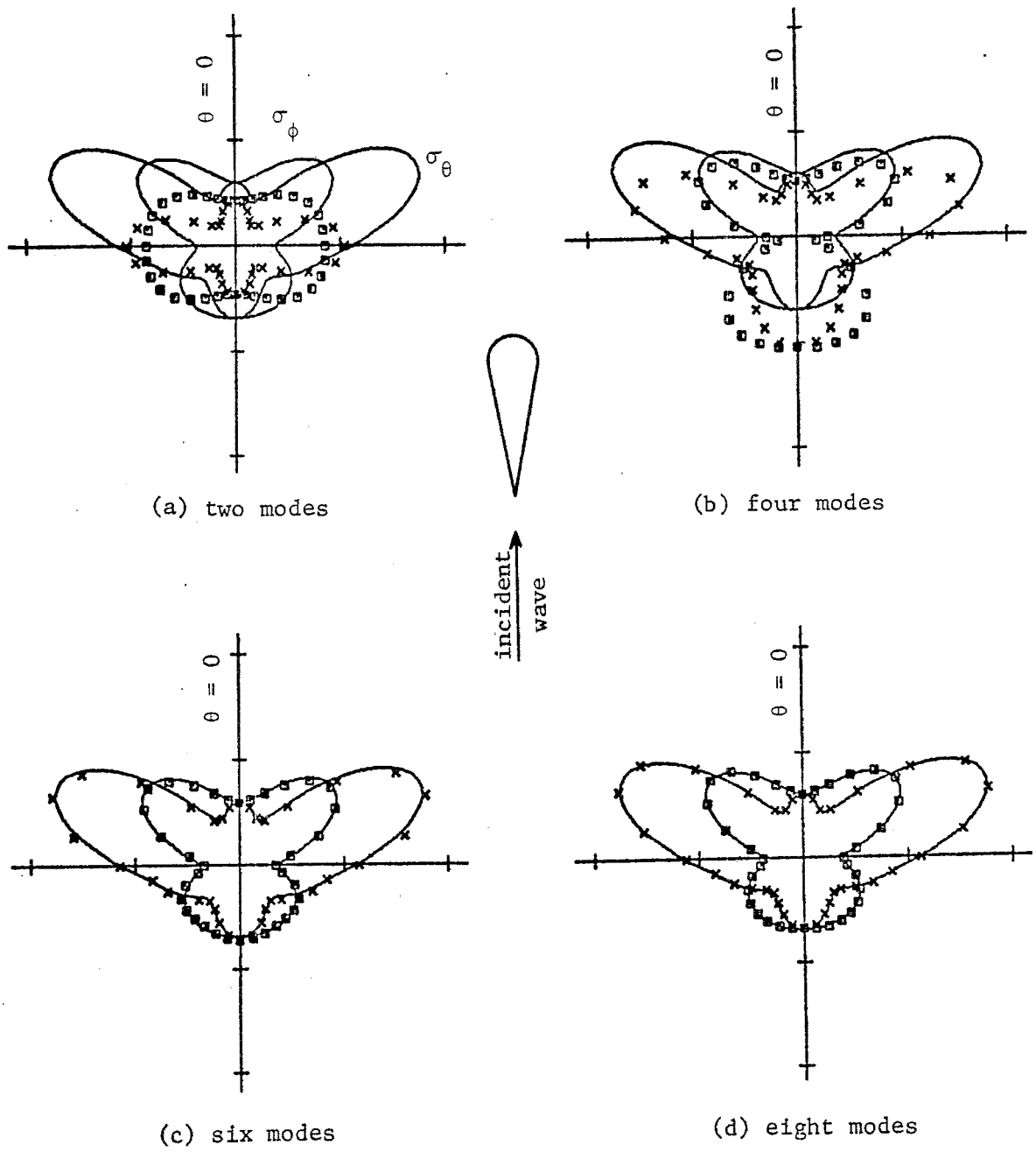

Fig. 2-8. Convergence of the modal solution for scattering by a cone-sphere excited by an axially incident plane wave. Solid curves are the matrix inversion solution, σ_θ being the E-plane pattern and σ_ϕ the H-plane pattern. The x's and squares are the corresponding modal solutions.

all excited. If the body is electrically small in diameter (say less than one-quarter wavelength, only the n=0 and n=1 modes contribute significantly to the scattering pattern. Similarly, in an aperture antenna problem, if the excitation is not rotationally symmetric, modes other than n=0 modes will be excited. Again, if the body is of electrically small diameter, usually only the n=0 and n=1 modes contribute significantly to the radiation pattern.

VII. APPLICATION TO WIRE OBJECTS

A computer program for the computation of the generalized impedance matrix of wire bodies of arbitrary shape is available [9]. This impedance matrix can be used in a slightly modified version of the bodies of revolution mode program of Part 3 to obtain the characteristic currents and fields of wire objects. A discussion of the method and some representative computations are given in this section.

A wire in space is specified by a number of points along its axis, plus its diameter. There may be more than one wire present, and these wires may have free ends, may be closed on themselves, or may be joined together. The expansion functions and testing functions are the same (Galerkin's method), and are chosen to be triangle functions extending over four subsections of the wire. For expansion, the triangles are approximated by four pulses, and for testing they are approximated by four impulses. Because of these approximations, the impedance matrix is not exactly symmetric, as it should be. It is made symmetric by averaging corresponding off diagonal impedance elements.

Computations of characteristic currents and characteristic fields have been made for a number of wire objects, and these modes have been used in modal solutions to demonstrate convergence in radiation and scattering problems. As an example, consider the wire arrow shown in the central insert of Figure 2-9. The parameter "a" is 0.25 wavelength, and the wire diameter is .004 wavelength. The graphs of Figure 2-9 show the six lowest order characteristic currents, plotted as a function of the contour variable, starting at the tip and ending at the tip. Note that the modes are either symmetric (even) or asymmetric (odd) about the mid-point with respect to the wire length variable. This could be predicted from the symmetry of the geometry of the wire. We did not use

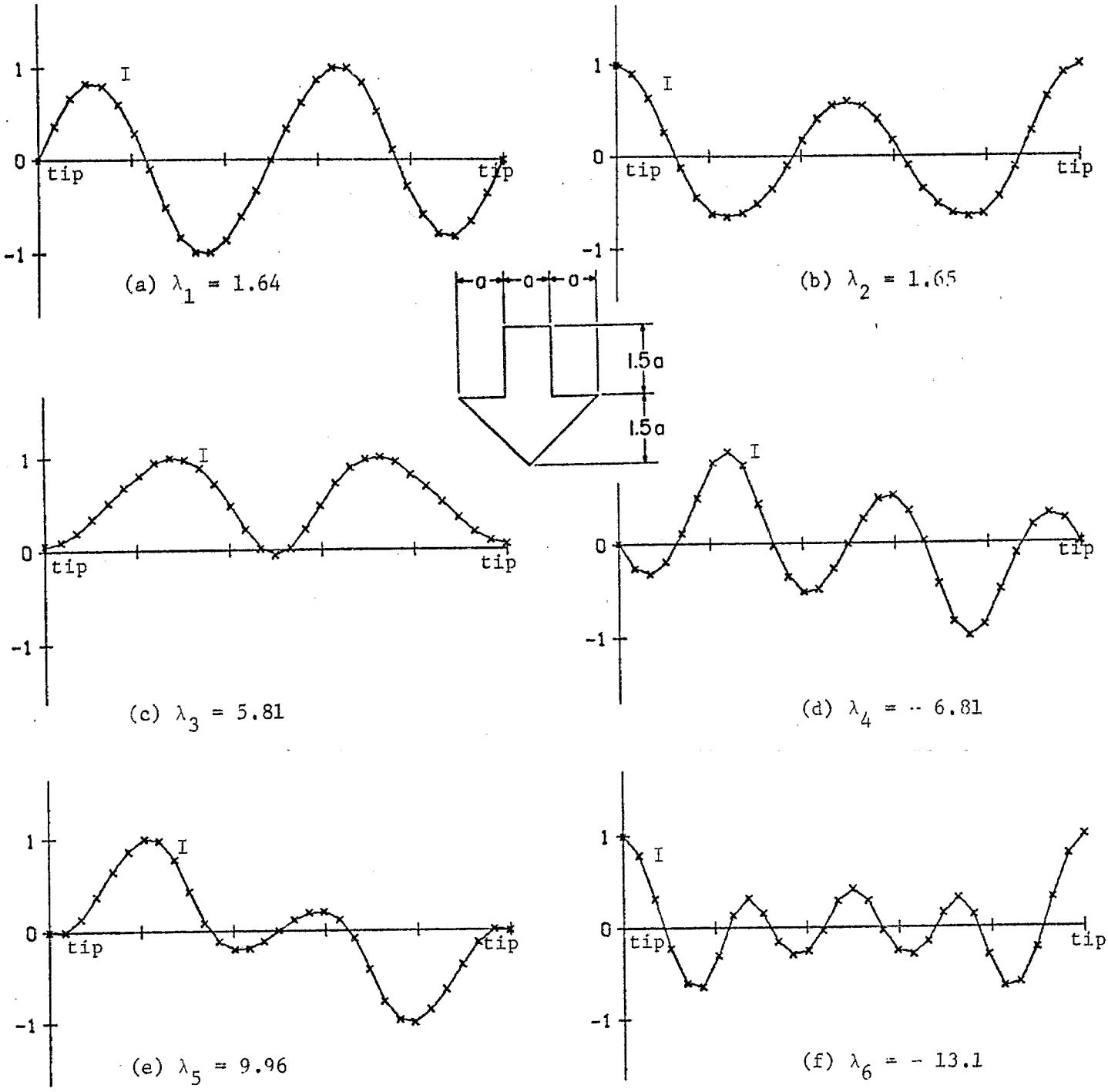

Fig. 2-9. Characteristic currents for the wire arrow, with "a" 0.25 wavelength and wire diameter 0.004 wavelength. The six lowest order modes are shown.

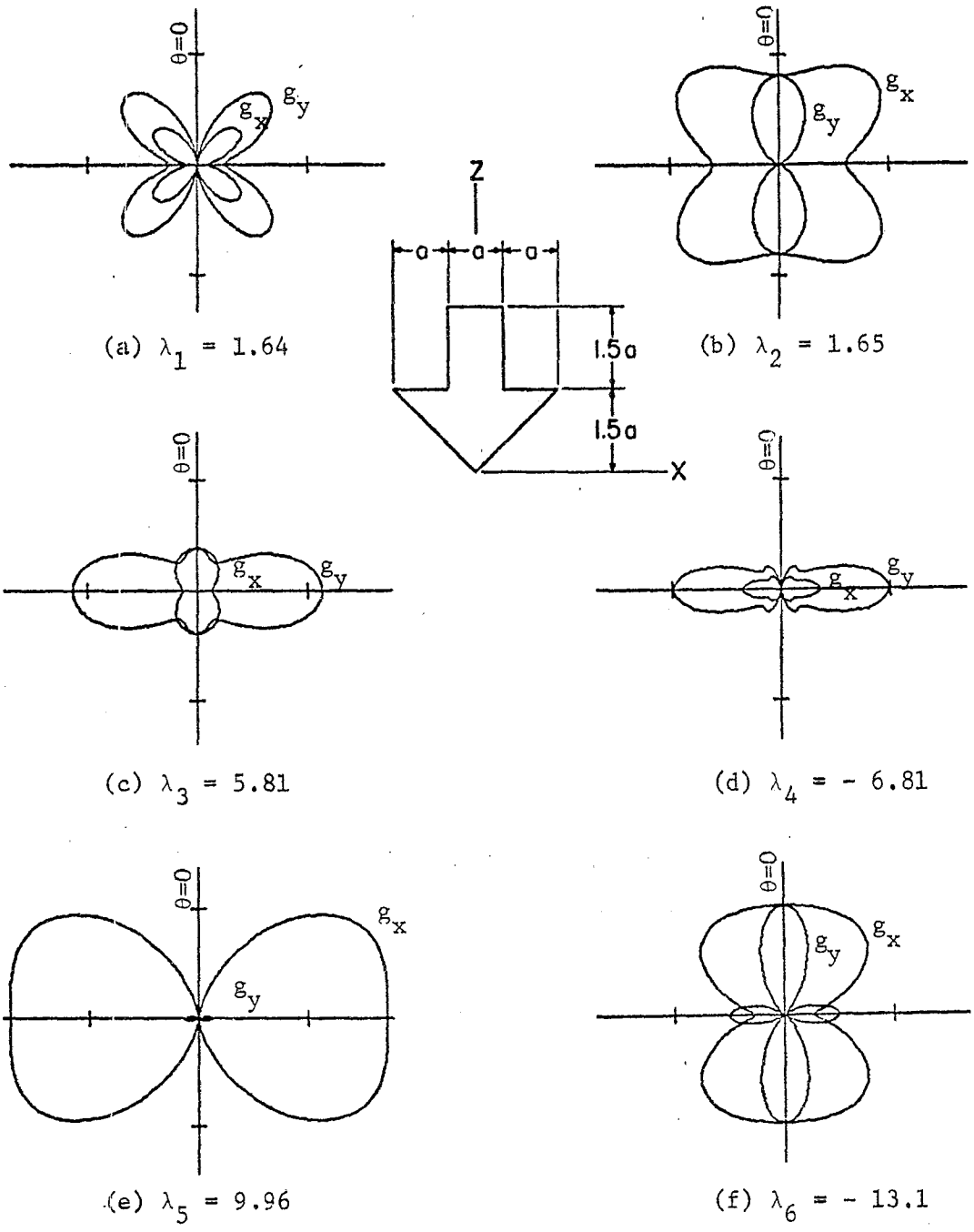

Fig. 2-10. Characteristic gain patterns for the wire arrow, with "a" 0.25 wavelength and wire diameter 0.004 wavelength. Patterns in the x=0 plane are labeled g_x, those in the y=0 plane g_y. The six lowest order modes are shown.

this symmetry in the computations because the program is written for objects of arbitrary shape. The currents were normalized by choosing their maximum amplitude to be unity.

Figure 2-10 shows the characteristic gain patterns for the six lowest order characteristic fields of the wire arrow. The arrow is considered to lie in the x-z plane, with its axis along the z axis. The two patterns shown are the gain in the x=0 plane (labeled g_x) and the gain in the y=0 plane (labeled g_y). The g_y pattern is always θ-polarized, and the g_x pattern is ϕ-polarized for even currents and θ-polarized for odd currents. The scale is linear, with each interval between tic marks representing an increment of two in gain. The gain patterns in other planes, such as the x-y plane, are not simply related to those in the x-z and y-z planes. For complete information, some sort of three-dimensional presentation of the gain patterns would be desirable.

Modal solutions for wire antennas and wire scatterers were also made and compared to the matrix inversion solution [6,9]. As modes were added, the modal solution converged to the matrix inversion solution in about the same way as for bodies of revolution. In the antenna problem, given a voltage source at some point along the wire, the modes are excited in proportion to their current amplitudes at the point of excitation. By using several voltage sources at several points, the excitation of a number of modes could be completely controlled. In the scattering problem, the excitation of modes could be controlled by placing lumped loads along the wire. However, if the loads were restricted to be passive, only partial control of the mode excitation would be possible.

VIII. DISCUSSION

The method of computing characteristic modes developed in this report can be used for conducting bodies of arbitrary shape, provided the body is not electrically large. General computer programs for determining the modes of bodies of revolution, and for using them in modal solutions for antenna and scattering problems, will be given in a later report. Computer programs for determining the generalized impedances for wires of arbitrary shape are also available [9]. Computer programs for bodies of arbitrary shape have not been written, primarily because of the difficulty of specifying coordinates on a three-dimensional surface S.

The characteristic currents are relatively easy to graph because they are real and exist on a surface. For example, on bodies of revolution there are at most two real components J_t and J_ϕ which, for each $\cos n\phi$, $\sin n\phi$ variation, can be expressed as a function of the single contour length variable. Similarly, on wire objects, there is a single real current I which is a function of the wire length variable. In contrast, the characteristic fields are complex and defined over three-dimensional space. Even on the radiation sphere we have four real functions to describe, namely, the real and imaginary parts of E_θ and E_ϕ. In this report we have plotted mode patterns in terms of $g = |E_\theta|^2$ or $g = |E_\phi|^2$, which shows only part of the picture. For example, note that all plots of g are symmetrical about $\theta = \pi/2$, even though the bodies do not have the corresponding symmetry. However, the field components E_θ and E_ϕ do not have this symmetry. For example, for bodies of revolution, $E_\theta(\pi-\theta) = (-1)^n E_\theta^*(\theta)$ and $E_\phi(\pi-\theta) = (-1)^{n+1} E_\phi^*(\theta)$. All such information is, of course, included in the general computer output, and could be plotted if desired.

The characteristic modes of bodies of arbitrary shape have most of the properties of the classical spherical modes, and can be used in much the same way. Because of their orthogonality properties, they are convenient to use for problems of analysis, synthesis and optimization of radiation and scattering. Now that we have an efficient way of calculating these modes, the theory can be applied to practical problems involving antennas and scatterers of arbitrary shape.

REFERENCES

(1) R.J. Garbacz, "A Generalized Expansion for Radiated and Scattered Fields," Interaction Note 180, 1968.

(2) R.J. Garbacz, "Modal Expansions for Resonance Scattering Phenomena," Proc. IEEE, vol, 53, No. 8, August 1965, pp. 856-864.

(3) R.H. Turpin, "Basis Transformation, Least Square, and Characteristic Mode Techniques for Thin-Wire Scattering Analysis," Interaction Note 181, 1969.

(4) R.J. Garbacz and R. Wickliff, "Introduction to Characteristic Modes for Chaff Applications," Technical Report 2584-6, Contract F33615-68-C-1252, Air Force Avionics Lab., Wright-Patterson A.F.B., Ohio.

(5) R.F. Harrington, "Time-Harmonic Electromagnetic Fields," McGraw-Hill Book Company, 1961.

(6) R.F. Harrington, "Field Computation by Moment Methods," The Macmillan Company, 1968.

(7) G.G. Montgomery, R.H. Dicke, and E.M. Purcell, "Principles of Microwave Circuits," Rad. Lab. Series, vol. 8, McGraw-Hill Book Company, 1948.

(8) J.R. Mautz and R.F. Harrington, "Radiation and Scattering from Bodies of Revolution," Appl. Sci. Res., vol. 20, June 1969, pp. 405-435.

(9) H.H. Chao and B.J. Strait, "Computer Programs for Radiation and Scattering by Arbitrary Configurations of Bent Wires," Interaction Note 191, September 1970.

(10) J.H. Wilkinson, "The Algebraic Eigenvalue Problem," Clarendon Press, Oxford, 1967, p. 34.

(11) A. Ralston and H. Wilf, "Mathematical Methods for Digital Computers," John Wiley and Sons, vol. I, 1969, Chap. 7, and vol. II, 1967, Chap. 4.

(12) Program given in Communications of the ACM, vol. 11, No. 12, December 1968, pp. 820-826.

(13) R.F. Harrington and J.R. Mautz, "Radiation and Scattering from Bodies of Revolution," Interaction Note 188, July 1969.

(14) IBM System/360 Scientific Subroutine Package (360A-CM-03X) Version III, Programmer's Manual.

APPENDIX A

UNWEIGHTED MODES

If we are interested only in diagonalizing the impedance operator, then any choice of weight operator M in (1-10) will do. The case M=I, the identity operator, is considered in this appendix. Then (1-10) becomes the unweighted eigenvalue equation

$$Z\vec{J}_n = \zeta_n \vec{J}_n \tag{A-1}$$

where ζ_n are eigenvalues and $\vec{J}_n$ are eigenfunctions. With respect to the symmetric product, we still have the orthogonality relationships

$$\oiint_S \vec{J}_m \cdot Z\vec{J}_n ds = 0 , \quad m \neq n \tag{A-2}$$

However, the mode currents are usually not real, and we lose orthogonality with respect to the Hermitian product (except in the special case of a sphere).

Only orthogonality of the type (A-2) is needed to diagonalize the impedance operator, and hence solutions similar to (1-30) remain valid. For example, we have a modal solution

$$\vec{J} = \sum_n \frac{\vec{J}_n}{Z_{nn}} \oiint_S \vec{J}_n \cdot E^i ds \tag{A-3}$$

where Z_{nn} is the modal impedance

$$Z_{nn} = \oiint_S \vec{J}_n \cdot Z\vec{J}_n ds \tag{A-4}$$

The admittance operator also continues to have a spectral representation of the form of (1-54), with $1+j\lambda_n$ replaced by Z_{nn}.

What has been lost by using the unweighted eigenvalue equation is orthogonality of the radiation patterns over the sphere at infinity, that is,

$$\oint\!\!\oint_{S_\infty} \mathbf{E}_m^* \cdot \mathbf{E}_n \, ds \neq 0 \qquad \text{(A-5)}$$

for $m \neq n$ (except in the special case of a sphere). This means that the radiation pattern computed from an unweighted modal solution is no longer a least-squares approximation to the true radiation pattern. Hence, we should expect a slower rate of convergence to the radiation pattern when unweighted modes are used than when the weighted modes are used.

For computation, the operator equation (A-1) was reduced to a matrix equation by techniques similar to those of Part 2, Section III. Characteristic currents for the unweighted modes were computed using a complex version of the Jacobi method for general matrices.* Figures A-1 and A-2 give some results for the unweighted eigenvalues and mode currents of a cone-sphere with 10° half cone angle, 0.4 wavelength sphere diameter, and 1.36 wavelengths total length. Figure A-1 shows the rotationally symmetric (n=0) modes, which can be compared to the corresponding weighted modes of Fig. 2-2. Figure A-2 shows $\cos\phi$, $\sin\phi$ (n=1) modes, which can be compared to the corresponding weighted modes of Fig. 2-4. Figure A-3 illustrates convergence of the unweighted modal solution for the radiation gain pattern, compared to the matrix inversion solution, as the number of modes are increased. The illustration of convergence for the corresponding weighted modal solution is Fig. 2-8. Note the much faster rate of convergence of the weighted modal solution, due to its least-squares approximation property.

---

*P. J. Eberlein, "A Jacobi-like Method for the Automatic Computation of Eigenvalues and Eigenvectors of an Arbitrary Matrix," Journ. S.I.A.M., vol. 10, No. 1, March 1962, pp. 74-88.

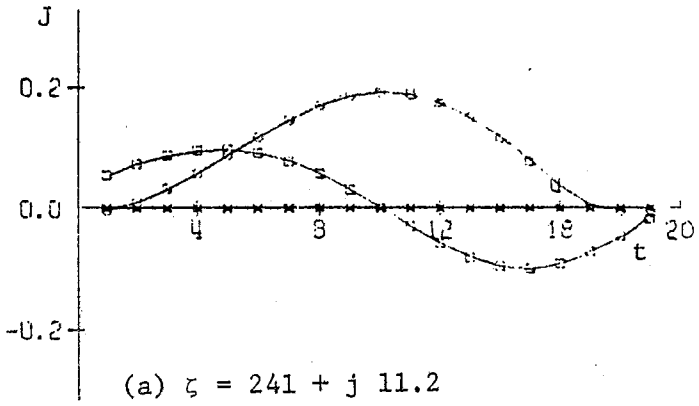

(a) ζ = 241 + j 11.2

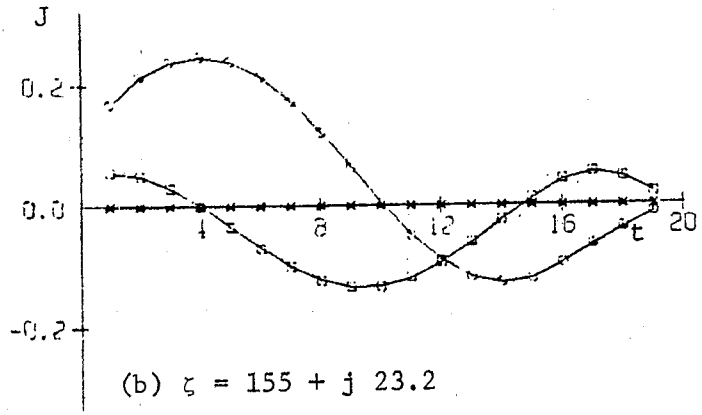

(b) ζ = 155 + j 23.2

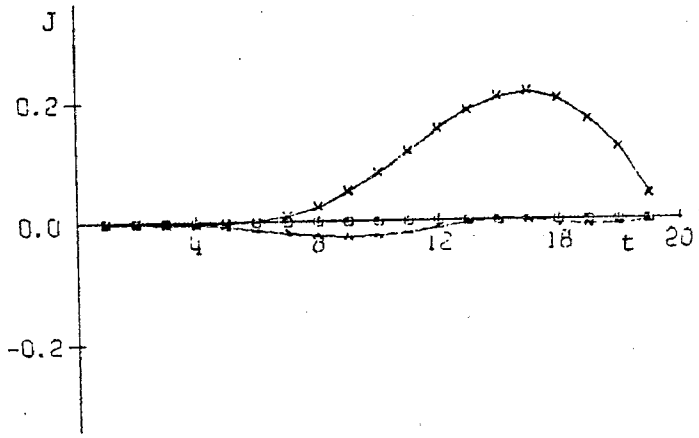

(c) ζ= 102 + j 216

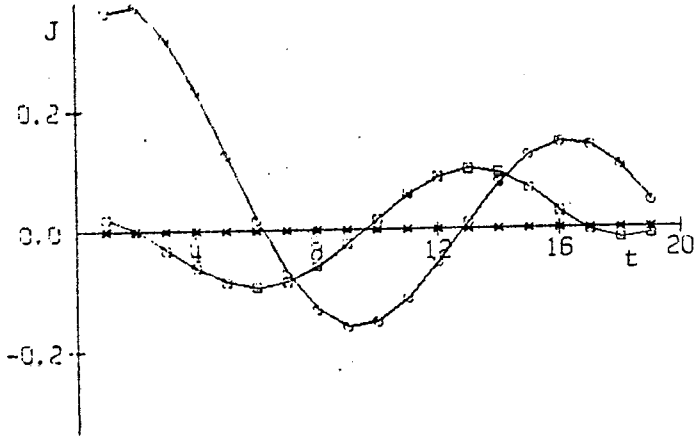

(d) ζ = 67.6 - j 60.4

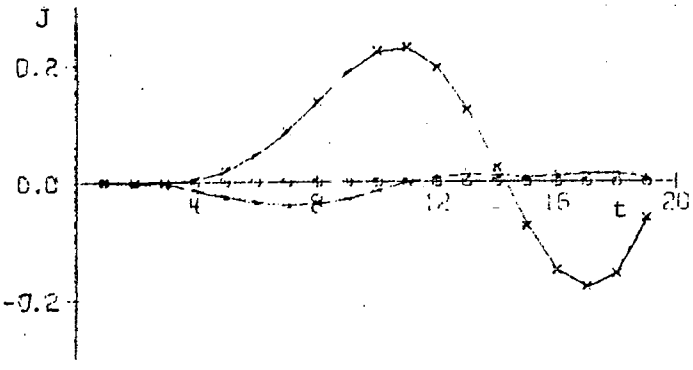

(e) ζ = 26.4 + j 165

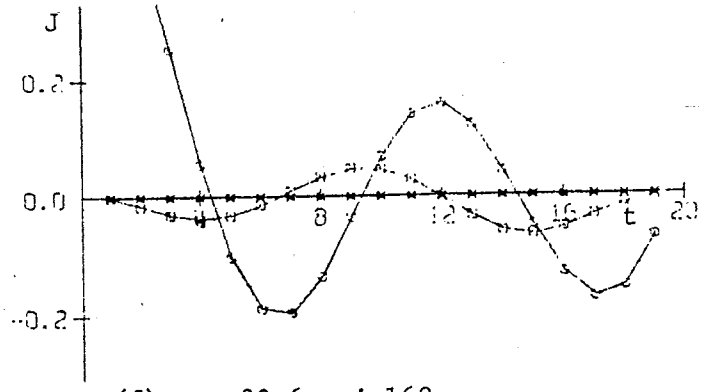

(f) ζ = 20.6 - j 168

Fig. A-1. Unweighted eigencurrents for the cone-sphere of Fig. 2-2 (10° half cone angle, 0.4 wavelength sphere diameter, 1.36 wavelengths total length), n=0 modes, Re J_t o o o , Im J_t □ □ □ , Re J_ϕ × × ×, Im J_ϕ △ △ △.

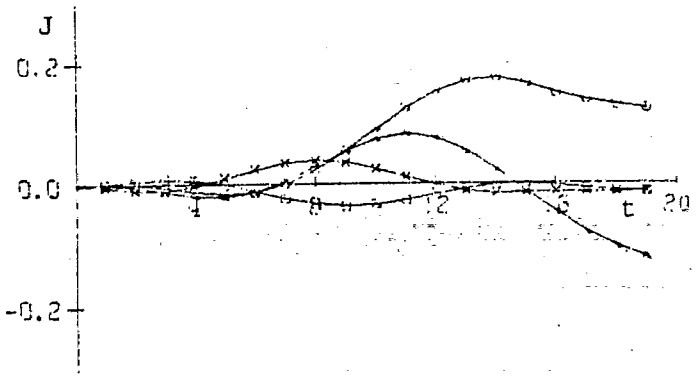

(a) ζ = 122 + j 210

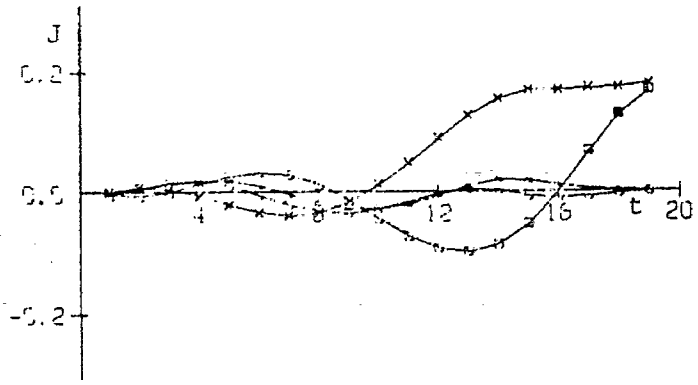

(b) ζ = 105 - j 152

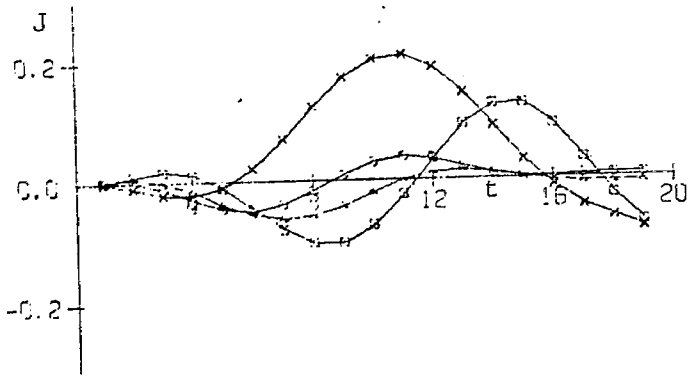

(c) ζ = 60.0 - j 193

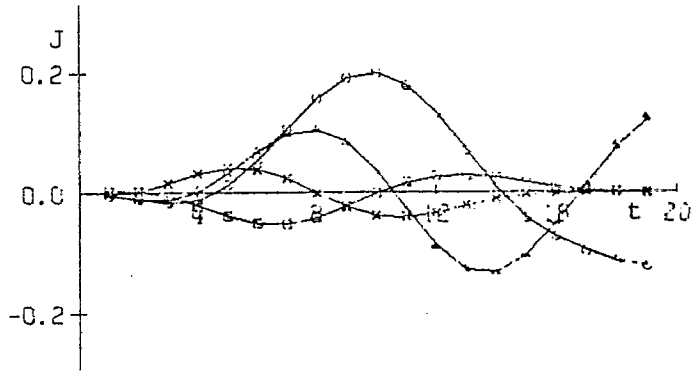

(d) ζ = 41.3 + j 167

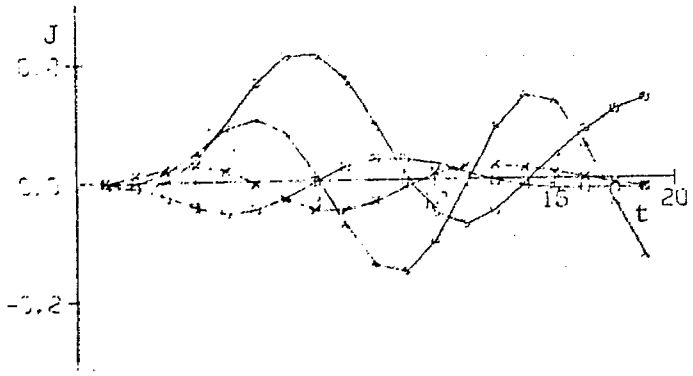

(e) ζ = 11.4 + j 127

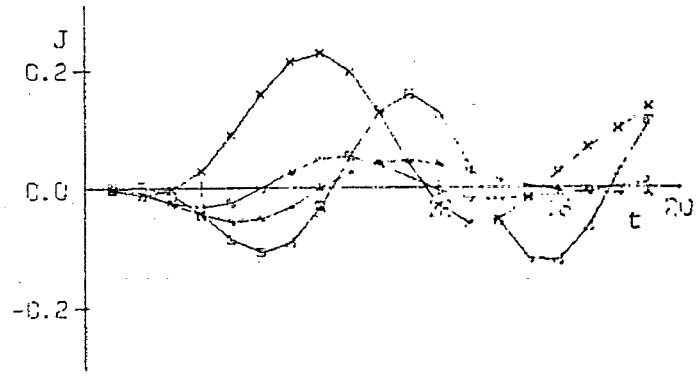

(e) ζ = 30.1 - j 268

Fig. A-2. Unweighted eigencurrents for the cone-sphere of Fig. 2-4 (10° half cone angle, 0.4 wavelength sphere diameter, 1.36 wavelengths total length), n=1 modes, Re J_t o o o, Im J_t □ □ □, Re J_ϕ × × ×, Im J_ϕ △ △ △.

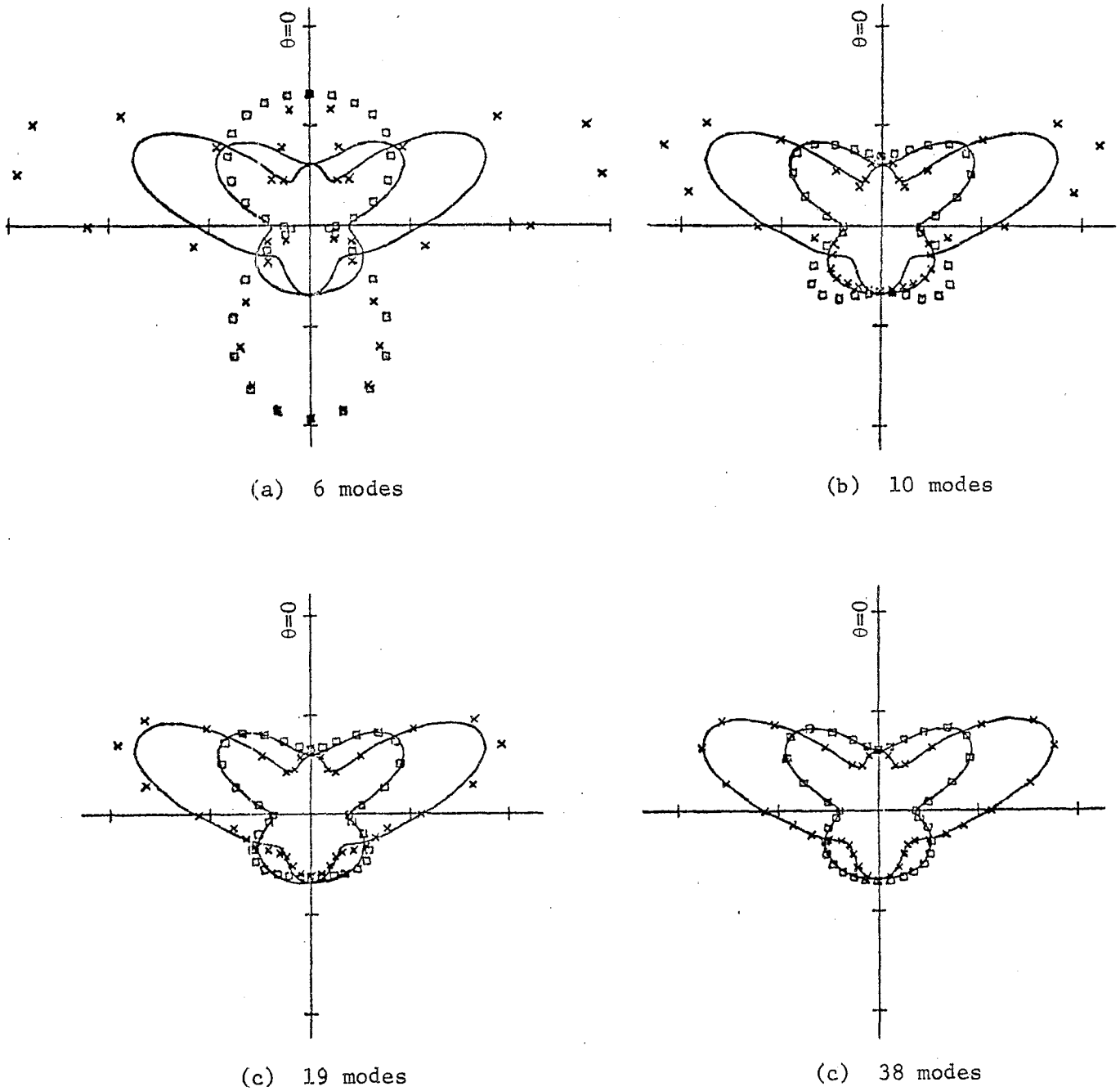

(a) 6 modes

(b) 10 modes

(c) 19 modes

(c) 38 modes

Fig. A-3. Convergence of the unweighted modal solution for scattering by the cone-sphere of Fig. 2-8 (10° half cone angle, 0.4 wavelength sphere diameter, 1.36 wavelengths total length) excited by a plane wave axially incident from $\theta = \pi$.

APPENDIX B

COMPUTATIONS FOR A SPHERE

To check the accuracy of our general computer program, we used it to compute the eigenvalues and eigencurrents for a conducting sphere, and compared them to the exact eigenvalues

$$\lambda_{nm}(TE) = -\frac{\hat{J}_m(ka)}{\hat{N}_m(ka)}$$

$$\lambda_{nm}(TM) = -\frac{\hat{J}'_m(ka)}{\hat{N}'_m(ka)} \tag{B-1}$$

and the exact eigencurrents

$$\vec{J}_{nm}(TE) = -\vec{u}_\theta \frac{n \cos n\phi}{\sin \theta} P_m^n(\cos \theta) + \vec{u}_\phi \sin n\phi \frac{\partial}{\partial \theta} P_m^n(\cos \theta)$$

$$\vec{J}_{nm}(TM) = -\vec{u}_\theta \cos n\phi \frac{\partial}{\partial \theta} P_m^n(\cos \theta) + \vec{u}_\phi \frac{n \sin n\phi}{\sin \theta} P_m^n(\cos \theta) \tag{B-2}$$

Here $\hat{J}_n$ and $\hat{N}_n$ are spherical Bessel functions, P_m^n is the associated Legendre polynomial, and a is the radius of the sphere. Equations (B-1) and (B-2) can be derived using the conventional spherical mode theory.*

Figures B-1 and B-2 show the eigenvalues and eigencurrents for the lowest-order modes of a conducting sphere of 0.4 wavelengths diameter. The n=0 modes are shown in Fig. B-1, the n=1 modes in Fig. B-2(a) to (d) and the n=2 modes in Fig. B-2(e) and (f). In each case the exact solution is shown solid, and the approximate solution is indicated by x's and squares. Both the exact and approximate mode currents are normalized so that

$$\frac{1}{S} \oiint_S |\vec{J}|^2 ds = 1 \tag{B-3}$$

Note that the accuracy of the approximate solution tends to decrease as the mode order increases.

---

*R. F. Harrington, "Time-Harmonic Electromagnetic Fields," McGraw-Hill Book Co., New York, 1961, Chapter 6.

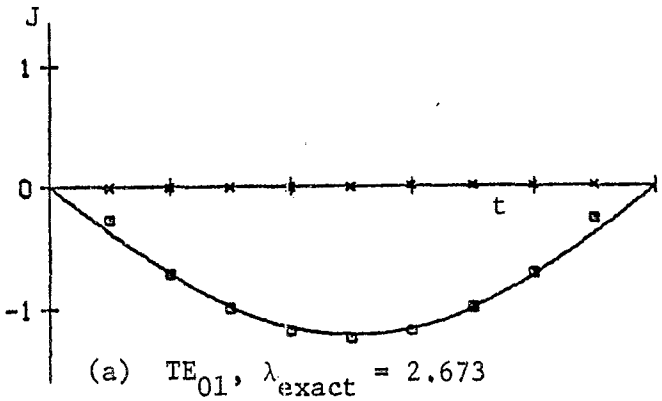

(a) TE_{01}, $\lambda_{exact} = 2.673$
$\lambda_{approx} = 2.682$

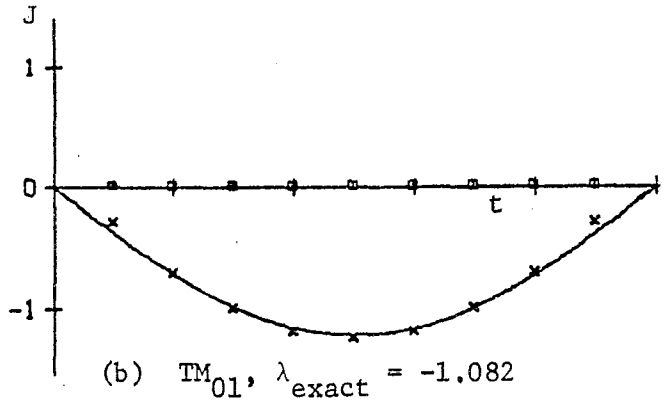

(b) TM_{01}, $\lambda_{exact} = -1.082$
$\lambda_{approx} = -1.096$

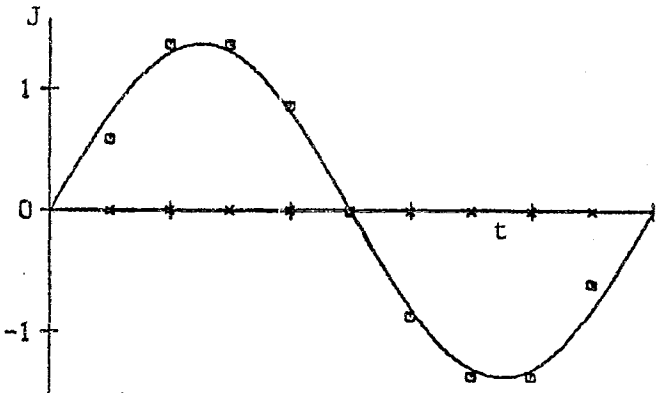

(c) TE_{02}, $\lambda_{exact} = 21.60$
$\lambda_{approx} = 21.82$

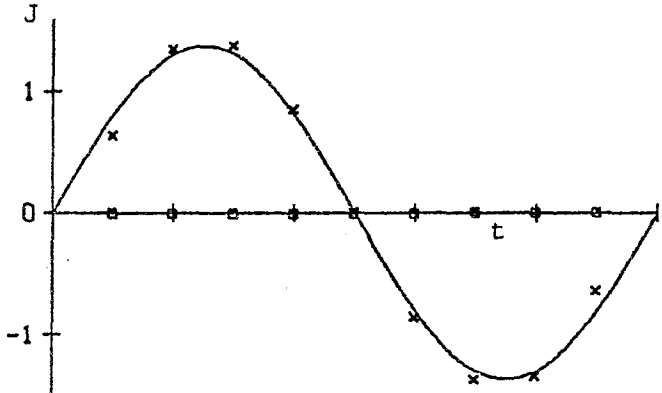

(d) TM_{02}, $\lambda_{exact} = -11.00$
$\lambda_{approx} = -11.60$

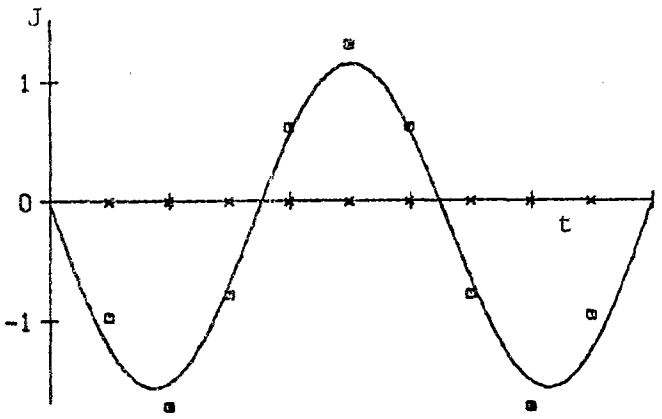

(e) TE_{03}, $\lambda_{exact} = 411.4$
$\lambda_{approx} = 468.8$

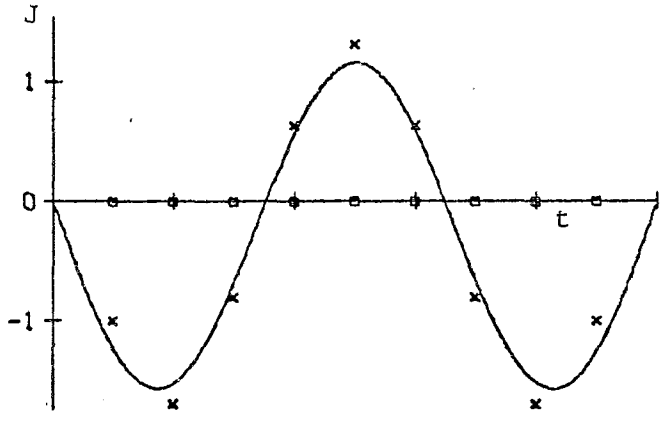

(f) TM_{03}, $\lambda_{exact} = -284.4$
$\lambda_{approx} = -290.7$

Fig. B-1. Characteristic currents for a conducting sphere of diameter 0.4 wavelengths, n=0 modes, exact solution solid, approximate J_t □ □ □, approximate J_ϕ × × ×.

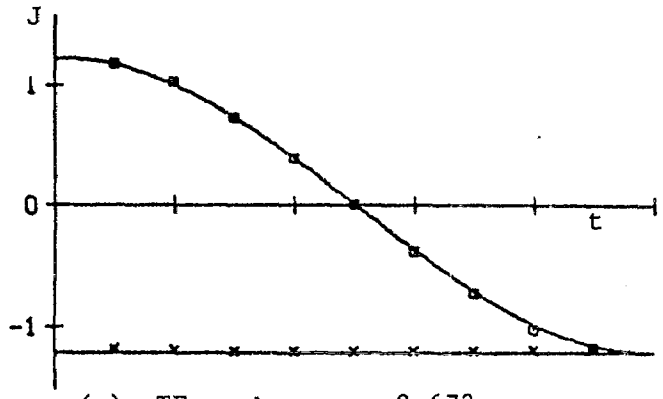

(a) TE_{11}, $\lambda_{exact} = 2.673$
$\lambda_{approx} = 2.683$

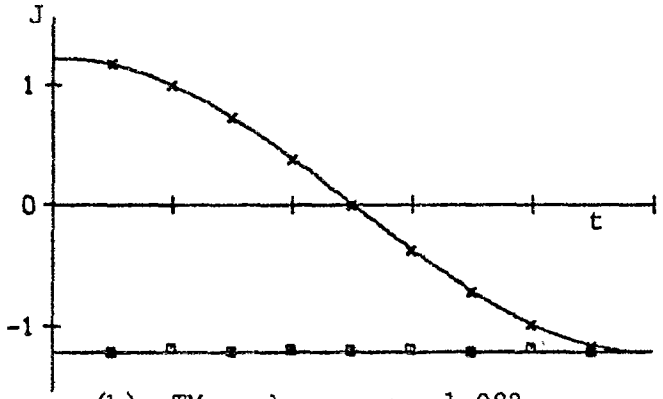

(b) TM_{11}, $\lambda_{exact} = -1.082$
$\lambda_{approx} = -1.085$

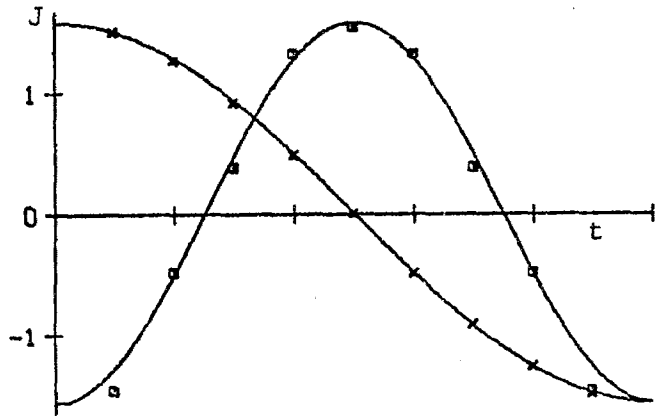

(c) TE_{12}, $\lambda_{exact} = 21.60$
$\lambda_{approx} = 21.66$

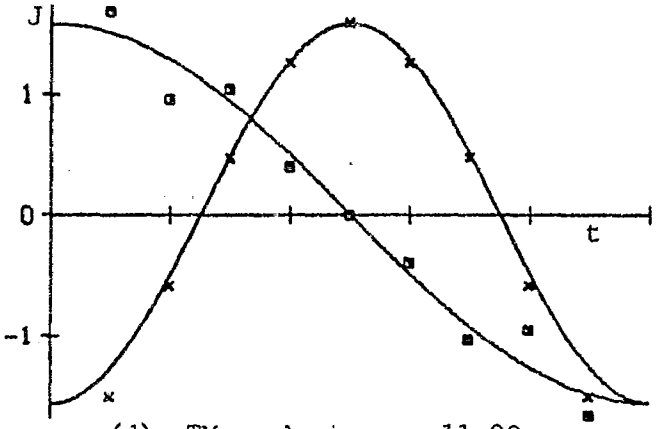

(d) TM_{12}, $\lambda_{exact} = -11.00$
$\lambda_{approx} = -11.30$

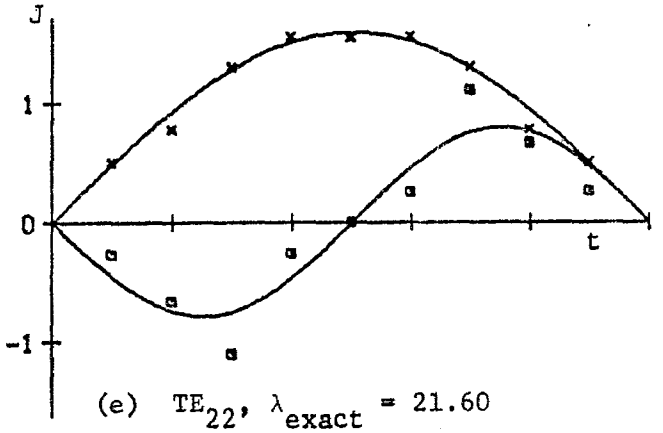

(e) TE_{22}, $\lambda_{exact} = 21.60$
$\lambda_{approx} = 21.56$

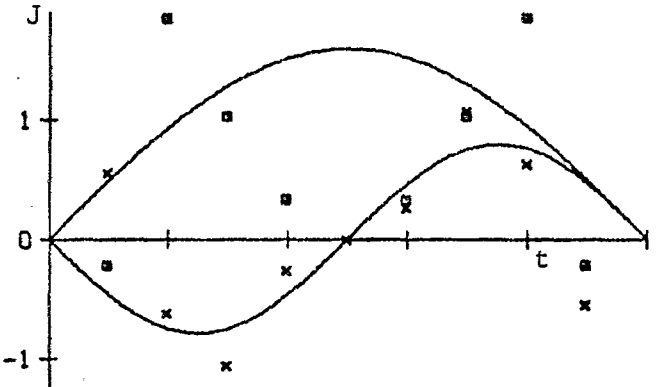

(f) TM_{22}, $\lambda_{exact} = -11.00$
$\lambda_{approx} = -11.26$

Fig. B-2. Characteristic currents for a conducting sphere of diameter 0.4 wavelengths, n=1 and n=2 modes, exact solution solid, approximate J_t □ □ □, approximate J_ϕ × × ×.